8-2013

Characterization of a glycosyphosphatidylinositol anchor transamidase in Arabidopsis thaliana and the function of GPI anchored proteins in stomatal development

Mark Gerald Ronald Bundy
mbundy1@utk.edu

To the Graduate Council:

I am submitting herewith a thesis written by Mark Gerald Ronald Bundy entitled "Characterization of a glycosyphosphatidylinositol anchor transamidase in Arabidopsis thaliana and the function of GPI anchored proteins in stomatal development." I have examined the final electronic copy of this thesis for form and content and recommend that it be accepted in partial fulfillment of the requirements for the degree of Master of Science, with a major in Biochemistry and Cellular and Molecular Biology.

Elena Shpak, Major Professor

We have read this thesis and recommend its acceptance:

Brad Binder, Albrecht Von Arnim

Accepted for the Council:
Dixie L. Thompson

Vice Provost and Dean of the Graduate School

(Original signatures are on file with official student records.)

Characterization of a glycophosphatidylinositol anchor transamidase in Arabidopsis thaliana and the function of GPI anchored proteins in stomatal development

A Thesis Presented for the
Master of Science
Degree
The University of Tennessee, Knoxville

MARK GERALD RONALD BUNDY
AUGUST 2013

ACKNOWLEDGEMENTS

I would like to start off by thanking my parents, Kevin and Mary Bundy. Without their love and support none of this would have ever been possible. Dr. Elena Shpak, thank you for taking a chance on me four years ago and accepting me into your lab. I appreciate all that you have done for me. You have not only taught me an array of scientific techniques but, more importantly, how to think critically. My committee, Dr. Brad Binder and Dr. Albrecht von Arnim, thank you for your continued advice and support. Dr. Todd Reynolds, for all of your help, advice, and patience as you taught me how to grow yeast and dissect tetrads. Tom Masi, I greatly appreciated your kind gift of p426 GPD, various reagents, and all of our discussions. Dr. Andreas Nebenführ, thank you for your gift of pAN456 and all your thoughtful insights on my project. Dr. Wolfgang Lukowitz, Thank you for your gift of CA-YDA. To the Shpak lab's past and present members, Allie Willet, Anastasia Aksenova, William Howell, Dr. Danyu Kong, Dr. Rucha Karve, Rebecca Wilson, Marshall Collins, Jennifer Baker, Pawel Kosentka, and Dr. Ming-Kun Chen, you have all helped me in more ways than one and I have appreciated working with everyone one of you. Rand Fugate, thank you for the programming and the funny comic strips. To my loving wife, Jessica, thank you for everything. Without your love, support, and understanding I would have lost my mind somewhere along the way. To my sister Christine, thanks for a being a pipsqueak. Finally, Morgan and Kieryn, daddy is coming home.

This project was funded by NSF grant IOS-0843340.

ABSTRACT

In plants stomata play a vital role for survival by allowing the gas exchange of CO_2 [carbon dioxide] and water vapor to occur. A stoma is a central pore flanked by two kidney shaped guard cells and in wild type there is at least one pavement cell between each stoma. The *ERECTA (ER)* gene family consisting of *ER, ERL1, ERL2* is involved in regulation of stomata development, where a triple mutant of *er erl1 erl2* displays an increased stomata index and clusters of stomata that disobey the one cell spacing rule. To better understand the pathway of stomata development, we performed an ethyl methanesulfonate (EMS) screen in an enhancer *erl1 erl2* background and looked for mutants with stomata clustering. A mutant with a strong stomata clustering phenotype was found and through map-based cloning the gene was identified as At1g08750 (renamed *AtGPI8*), a putative glycosylphosphatidylinositol-anchor (GPI) transamidase (GPI-T). In mammals and yeast the GPI-T is responsible for the cleaving of the C-terminal end of a protein and the attachment of the GPI anchor. Here we report the characterization of the partially functional *atgpi8-1* and the lethal knockout *atgpi8-2*. We demonstrate how GPI anchored proteins (GPI-APs) play a role in fertility, growth, plasmodesmata permeability and stomata development. Furthermore, we investigate the involvement of a GPI-AP in the stomata development pathway. Genetic interactions have determined that the *er* family acts synergistically with *atgpi8-1*. A gain of function mutant of YDA has epistasis over *atgpi8-1*. *Tmm* and *atgpi8-1* share similar phenotypes in leaves but *tmm* is epistatic over *atgpi8-1* in stems. These results indicated that a

GPI-AP protein functions upstream of YDA, and either downstream of or in concurrence with the ER family and TMM. Sequence analysis suggests that TMM could potentially be a GPI-AP in the stomata development pathway.

“Results! Why, man, I have gotten a lot of results. I know several thousand things that won’t work.”

- Thomas A. Edison

TABLE OF CONTENTS

Chapter 1 1
Introduction 1
Stomata Development 1
Stomatal Development Pathway 1
Receptors 2
Ligands 7
MAPK Signalling 10
Transcription Factors 12
Conclusions 16
GPI Anchors 18
Function of GPI anchors 19
GPI Anchor Biosynthesis 22
GPI anchor Transamidation 23
Gpi8p 25
GPI anchor signal 27
GPI-anchor remodeling and transport to Golgi apparatus 29
GPI anchor biosynthesis genes in plants 30
Select GPI anchored proteins in plants 33
Conclusions 34
Chapter 2 35
Materials and Methods 35
Plant Materials and Growth Conditions 35
Map Based Cloning of atgpi8-1 35
Sequence alignment 36
Crosses and Genotyping 38
Reverse Transcription PCR 39
Analysis of plant development and growth 40
Transient Transformation of Seedlings and Cell-to-Cell Mobility Assay 41
Plasmid Construction 41
Yeast transformation and tetrad dissection 42
Arabidopsis Genome Initiative 43
Chapter 3 44
Results 44
Positional cloning of *atgpi8-1* 44
Atgpi8-1 mutations affect many developmental processes 48
The *atgpi8-1* mutant has decreased plasmodesmata conductivity 51
Synergistic interactions of *ERf*s and *ATGPI8* during stomata development 54
The *tmm-1* mutation is epistatic to *atgpi8-1* mutation 59
Chapter 4 61
Discussion 61

GPI-APs are involved in fertility 61
GPI-APs are involved in root development 63
GPI–APs are involved in regulation of plasmodesmata permeability 64
GPI-APs are involved in stomata development 65
A new model system for the study of GPI anchors 70
Works Cited 72
Vita 87

LIST OF TABLES

Table 1 Homology of proteins involved in the GPI anchor biosynthesis 32
Table 2 SSLPs used to positionally clone *atgpi8-1* 37

LIST OF FIGURES

Figure 1.1 Stomata development pathway 4
Figure 1.2 ERf signalling pathway 17
Figure 1.3 Core structure of a GPI anchor. 20
Figure 1.4 Attachment of GPI anchors 24
Figure 1.5 The GPI-anchor signal sequence 28
Figure 3.1 Positional cloning of *AtGPI8-1* 45
Figure 3.2 The *atgpi8-1* mutation leads to formation of stomata clusters and is allelic with *atgpi8-2*. 47
Figure 3.3 Growth phenotypes of *atgpi8-1* plants. 49
Figure 3.4 Increased callose accumulation and decreased plasmodesmata conductivity of *atgpi8-1*. 53
Figure 3.5 Genetic interactions of *ERECTA* family genes and *AtGPI8* during stomata development. 55
Figure 3.6 CA-YDA and bikinin partially rescue epidermal phenotype of *atgpi8-1*. 58
Figure 3.7 The *tmm-1* mutation is epistatic to the *atgpi8-1* mutation 60

Chapter 1

Introduction

Stomata Development

Plants undergo photosynthesis and therefore must exchange gases with the environment, allowing the intake of CO_2 and the output of O_2 and H_2O through specialized pores in the plant's epidermis called stomata. A stoma is a central pore flanked on both sides by kidney shaped guard cells. The development of the stoma requires a series of predictable cell divisions and cell fate transitions. The different steps of the stomata development pathway have been well characterized, but the underlying molecular mechanism still is not completely understood.

Stomatal Development Pathway

All stomata are formed through a sequence of cell divisions and cell fate transitions (Fig1.1) (Bergmann and Sack, 2007; Pillitteri and Torii, 2012; Torii, 2012). The first step starts with a protodermal cell differentiating into a meristemoid mother cell (MMC). The MMC undergoes an asymmetric division with the smaller cell differentiating into a meristemoid and the bigger cell into a stomatal lineage ground cell (SLGC). From this point the meristemoid can either enter more rounds of asymmetric cell divisions, creating more MMCs and SLGCs, or it can undergo the next cell fate

transition into an oval guard mother cell (GMC). In either path, the meristemoid will eventually differentiate into a GMC. The GMC will then undergo symmetric division to form two guard cells (GCs). SLGCs will commonly differentiate into pavement cells, however, they are also able to undergo asymmetric division and form new MMCs. Through this entire process there is always at least one SLGC or a pavement cell between every GMC or a stoma complex. This spacing is referred to as the one cell spacing rule, in which every stoma has at least one pavement cell separating it from other stomata (Kagan and Sachs, 1991). When a leaf reaches maturity the stomatal development process ends, and it is hypothesized that a majority of the pavement cells produced in leaves are generated through the stomatal lineage pathway (Nadeau and Sack, 2002a).

Stomata development is regulated by the ER/TMM signaling pathway that includes plasma membrane bound receptors, ligands, MAPK signaling, and transcription factors.

Receptors

One of the main receptors in the stomatal development pathway is ERECTA (ER). *ER* encodes for a Leucine Rich Repeat Receptor-Like-Kinase (LRR-RLK) that contains twenty leucine rich repeats in the extracellular domain, a transmembrane domain, a juxtamembrane domain, and a Ser/Thr kinase domain. The first *er* mutant was described in the 1950s and this mutation is present in the well-studied ecotype Landsberg

er (Redei, 1962). Landsberg *erecta* is noted by its smaller size when compared to the other commonly used ecotype Columbia. Another mutant, *er-105,* was isolated in the Columbia background (Torii et al., 1996). The *er-105* mutant is distinguished by its compact inflorescence with clustered flower buds, short internodes, short pedicels, round flowers, short blunt siliques, and short plant height (Bowman, 1993; Torii et al., 1996). The *er* mutant has an increase in meristemoid formation and excessive asymmetrical division (Shpak et al., 2005). Localization of ER has been shown to be in the plasma membrane through biochemical fractionation (Lee et al., 2012). The *ER::ER-GFP* construct has not been a viable way to visualize ER localization through microscopy and only through *ER::Δkinase*-GFP has it been possible to see accumulation of ER in the plasma membrane (Shpak and Torii, unpublished). *ER::Δkinase* is a truncated ER without the kinase domain under the native promoter and terminator but it is expressed at a much higher level than endogenous protein (Shpak et al., 2003).

There are two partially redundant paralogues of *ER* named *ERECTA-LIKE-1* (*ERL1*) and *ERECTA-LIKE-2* (*ERL2).* Together the three genes make up the *ER* family (*ER*f). Single and double mutants of *erl1* and *erl2* have no distinguishable growth phenotype. Double mutants *er erl1* or *er erl2* have reduced plant height and decreased plant height and sterility (Shpak et al., 2004). Examination of the epidermis revealed a high stomatal index, with a high percentage of stomata found in clusters of two or more indicating that the three members of the *ER* family are redundant during stomata development (Shpak et al., 2005).

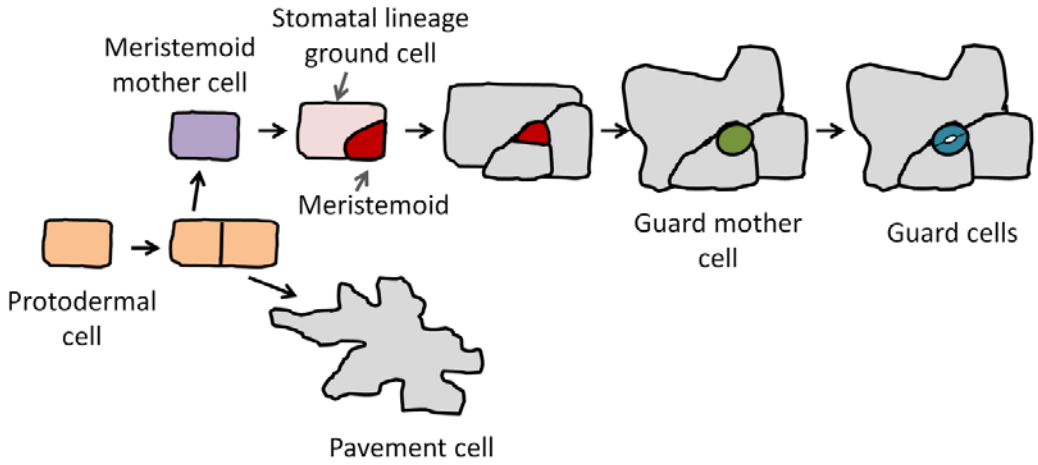

(Shpak, unpublished)

Figure 1.1 Stomata development pathway

Cells begin as protodermal cells (orange) and go through symmetrical division. They can either transition to pavement cells (grey) or MMCs (purple). The MMC will go through asymmetrical division to form a SLGC (pink) and a meristemoid (red). The meristemoid can undergo many rounds of asymmetrical division before transitioning into a GMC (green). The GMC will undergo symmetrical division to form two guard cells (blue).

One of the first genes discovered to affect stomatal development and patterning was *TOO MANY MOUTHS (TMM),* which encodes an LRR Receptor-Like-Protein (Nadeau and Sack, 2002b) and consists of a extracellular domain of 10 leucine rich repeats with either a transmembrane region (Nadeau and Sack, 2002b) or a putative GPI-anchor site (Borner et al., 2003) and no cytoplasmic domain (Nadeau and Sack, 2002b). The lack of a cytoplasmic domain suggests TMM acts as a modulator of stomata development by potentially binding to ligands and/or the ER family RLKs. The stomata phenotype of *tmm* is organ specific, with an increased stomatal density and large clusters of stomata being found in leaves, no stomata being found in stems, and a gradient of stomata being found in pedicles (Geisler et al., 1998; Yang and Sack, 1995). This difference suggests TMM has the ability to either promote stomata development (stems) or inhibit stomata development (leaves). Expression of TMM can be found in meristemoids, SLGCs, and GMCs but never in mature pavement cells (Nadeau and Sack, 2002b). Two forms of GFP fusions have been created with TMM under the native promoter, the first is a C-terminal fusion and the second is an N-terminal fusion (Nadeau and Sack, 2002b). Both are able to complement *tmm-1* phenotype, however the subcellular localization of GFP fluorescence seems to be slightly different in *TMM*::*GFP-TMM* plants. There is faint fluorescence of GFP along the outside edge of the cell, most likely representing the plasma membrane and the reduced fluorescence caused by the acidity of the extracellular space. The *TMM::TMM-GFP* plants have a brighter

fluorescence and GFP appears to be expressed in the endoplasmic reticulum as well as the along the edge of the cell (Nadeau and Sack, 2002b).

These observations support the model of TMM being GPI-anchored as the localization of GFP in *TMM::TMM-GFP* plants could represent GFP being cleaved during GPI anchor attachment to TMM and the GFP localization in the endoplasmic reticulum and the vacuole. The study of genetic interactions with the ER family identified that the *tmm er* mutant has the same phenotype as *tmm* in stems; the loss of *tmm, er* and *erl1* restores stomata to the stems, and the quadruple mutant *tmm er erl1 erl2* has a similar phenotype to *er erl1 erl2* with the epidermis of stems containing large clusters of stomata (Shpak et al., 2005). These observations reveal that as TMM promotes stomata development in stems the ER family inhibits stomata development and the two most likely work together to form a balance. Biochemical analysis of TMM, ER and ERL1 suggests that ER and ERL1 are able to form homodimers *in vitro* and *in vivo* where TMM is not. Furthermore ER and ERL1 are able to form heterodimers with each other and with TMM (Lee et al., 2012) giving support to the hypothesis that TMM acts as a modulator for the function of the ER family. One caveat to these results is the use of C-terminal tags on TMM. If TMM is GPI-anchored, as predicted, these results could either be an experimental artifact or they may not explain the entire story of TMM's function.

Ligands

With the discovery of the ER-family and TMM there began a search for possible ligands for these receptors. The first discovered ligand was EPIDERMAL PATTERNING FACTOR 1 (EPF1) (Hara et al., 2007). The overexpression of *EPF1 (EPF1-OX)* inhibits stomata development whereas loss of function *epf1* increases stomatal density and the percentage of stomata found in clusters of two or more (Hara et al., 2007). Analysis of *EPF1::GFP* transgenic plants suggests that EPF1 is expressed in meristemoids, GMCs and young GCs (Hara et al., 2007). *TMM*, *ER*, *ERL1* and *ERL2* are epistatic over *EPF1* indicating *EPF1* functions upstream of those receptors.

Through sequence similarity to *EPF1* ten other ligands were identified as potential ligands of ER family receptors, EPIDERMAL PATTERNING FACTOR 2 (EPF2) (Hara et al., 2009; Hunt and Gray, 2009) and nine EPIDERMAL PATTERNING FACTOR LIKE (EPL) proteins (Hara et al., 2009). One common elemental in this 11 member family is a c-terminal end with six to eight cysteines (Hara et al., 2009). The cysteines are possibly used to form disulfide bonds that are important for the structure and function of the peptides (Ohki et al., 2011).

Overexpression of *EPF2* leads to an epidermis void of meristemoids and stomata, indicating *EPF2* can blocks cells from entering the initial step to the stomata development pathway (Hara et al., 2009). Loss of function *epf2* also leads to increased stomatal density. Analysis of *EPF2::GFP* transgenic plants detects expression of EPF2 in protodermal cells, in meristemoids, SLGCs, and GMCs, but unlike EPF1 there is no

expression in GCs. There is also no expression in pavement cells (Hara et al., 2009). The double mutant *epf1 epf2* has a synergistic phenotype with a greater increase in stomatal density and the development of stomata in clusters of 3 or more (Hara et al., 2009). Analysis of genetic interactions shows that *er* has epistasis over *epf2* in all aboveground organs and *tmm* has epistasis over *epf2* in stems but not leaves (Hunt and Gray, 2009).

Biochemical analysis of EPF1 and EPF2 demonstrated direct binding to the ER-family and TMM *in vivo* (Lee et al., 2012). Co-immunoprecipitation, quartz crystal microbalance, and surface plasmon resonance experiments suggested that EPF1 binds to ER and ERL1 but not TMM, whereas EPF2 binds to ER, ERL1, and TMM, providing further evidence to support the model of EPF1 and EPF2 acting as regulators of different stages of stomata development through the ER-family. The preferential binding of EPF2 to TMM provides further insight into its function as a modulator of the ER-family activity.

A third member of the EPFL family, EPFL9 or *STOMAGEN*, is also involved in the regulation of stomata development. Besides its original identification through sequence similarity to *EPF1* (Hara et al., 2009) *STOMAGEN* was also identified *in silica* through a high coexpression coefficiency value with *TMM* and *EPF1* (Kondo et al., 2010; Sugano et al., 2010). Overexpression of *STOMAGEN* leads to an increased stomatal density and stomata clustering. Knocked down expression of *STOMAGEN* through RNAi (*STOMAGEN-RNAi)* leads to a severe reduction in stomatal density (Kondo et al., 2010;

Sugano et al., 2010). These two results indicate that *STOMAGEN* is a positive regulator of stomatal development. Expression of *STOMAGEN* has been shown through *STOMAGEN*::GUS and *STOMAGEN::GFP* to be in the mesophyll, a tissue responsible for photosynthesis (Kondo et al., 2010; Sugano et al., 2010). Similar to *EPF1* and *EPF2*, *STOMAGEN* requires *TMM* and at least one member of the *ER* family to function which supports its role in the *ER* signaling pathway (Kondo et al., 2010; Sugano et al., 2010). The double mutants *epf1 STOMAGEN-RNAi* and *epf2 STOMAGEN-RNAi* lead to a reduction in stomata density (Sugano et al., 2010)and endogenously applied *STOMAGEN* did not affect the stomatal density of *epf1 epf2* mutants (Kondo et al., 2010). STOMAGEN promotes stomatal development acting as an antagonist for TMM and/or the ER family while EPF1 and EPF2 inhibit stomatal development acting as agonists for the same receptors. The competition between the two sets of ligands for receptors could allow for a more controlled signaling pathway.

Another ligand involved in stomatal development is CHALLAH (CHAL) or EPF6. *CHAL* was discovered in a mutant screen based on mutants that rescued stomata formation in stems of *tmm* (Abrash and Bergmann, 2010). The triple mutants, *tmm chal erl1* or *tmm chal erl2*, have stomata on the stem but *tmm chal er* returns to having no stomata indicating that ER is required for CHAL function (Abrash and Bergmann, 2010). Overexpression of *CHAL* leads to reduced stomatal density in leaves in weak lines and no stomata in stronger lines (Abrash and Bergmann, 2010). Collectively those experiments

suggest that *CHAL* is a negative inhibitor of stomata development similar to *EPF1* and *EPF2*.

MAPK Signalling

The next downstream step in the signaling cascade involves the mitogen activated protein kinase kinase kinase (MAPKKK) YODA (YDA). *YDA* was originally discovered in a mutant screen searching for genes that affect early embryo development in *Arabidopsis* (Lukowitz et al., 2004). The phenotype of *yda* consists of a severely dwarfed plant with small rosette leaves, compact shoots, small sterile flowers (Lukowitz et al., 2004) and a large increase in stomatal density and a high number of stomata found in clusters, similar to *er erl1 erl2* and *tmm* with a large increase in stomatal density and a high number of stomata found in clusters (Bergmann, 2004). In many MAPKKKs, including YDA, the N-terminus acts as a negative regulatory domain and its removal creates a constitutively active form of the kinase (Kovtun et al., 2000; Lukowitz et al., 2004). The phenotype of constitutively active *YDA* (CA-YDA) is the opposite of *yda* and in the stronger transgenic lines, stomata formation is completely prevented (Bergmann, 2004) similar to the phenotype of *EPF1-OX*. Genetic interactions with *tmm* show that *CA-YDA/+* is able to rescue the *tmm* phenotype in cotyledons (Bergmann, 2004). This suggests YDA acts downstream of TMM and may potentially be a target for ER kinase

activity although to date there has been no evidence to show a direct phosphorylation between the ER family receptors and YDA.

Downstream of YDA are MKK4/MKK5 and MPK3/MPK6. *MPK3* and *MPK6* are redundant negative regulator's of stomata development. Single mutants have no distinguishable phenotype and double mutants are embryo lethal. Therefore, RNAi knockdown lines were used to analyze their effects on stomata development (Wang et al., 2007). In *mpk6 MPK3RNAi* knockdown lines seedlings that survived the embryo stage never lived past the cotyledon stage (Wang et al., 2007). The cotyledons had the distinguishable epidermal phenotype of stomata appearing in very large clusters and in some cases covering the entire epidermis (Wang et al., 2007). MKK4 and MKK5 are also functionally redundant negative regulators of stomata development (Wang et al., 2007). Single mutant RNAi lines of *MKK4RNAi* and *MKK5RNAi* displayed small clusters of two to three stomata and in *MKK4RNAi MKK5RNAi* plants once again arrested at the cotyledon stage and in some cases the entire epidermis of the cotyledon was made up completely of stomata (Wang et al., 2007). Constitutively active MKK4 and MKK5 behave in a similar manner to CA-YDA suppressing stomata development. Furthermore constitutively active MKK4 and MKK5 were able to partially rescue *yda* which suggests that MKK4 and MKK5 act downstream of YDA in the stomata development pathway (Wang et al., 2007).

Transcription Factors

There are a number of known transcription factors that act on different steps in the stomata lineage pathway. The transcription factors can be divided into two families, the first is basic Helix-Loop-Helix (bHLH) proteins and the second is R2R3 MYB proteins. The bHLH transcription factors involved in stomata development are SPEECHLESS (SPCH), MUTE, FAMA, SCREAM/ICE1 (SCRM) and SCRM2. The R2R3 MYB transcription factors are FOUR LIPS (FLP) and MYB88.

The first transcription factor involved in and required for the initiation of the stomata development pathway is SPCH. Mutants of *SPCH* either lack any stomata in the epidermis as in *spch-1* or have a severely reduced stomatal index as in *spch-2* and overexpression of *SPCH* leads to a large increase in entry divisions and therefore a large increase in stomatal density, including many stomata found in large clusters (MacAlister et al., 2007; Pillitteri and Torii, 2007). SPCH is expressed during early development in the protoderm and eventually becomes isolated in stomatal lineage cells (MacAlister et al., 2007; Pillitteri and Torii, 2007). The phenotype of *spch* is strikingly similar to that of *CA-YDA* indicating they could be acting in the same pathway which is further supported by the fact that *SPCH* is epistatic to *YDA* in regard to stomata development (MacAlister et al., 2007; Pillitteri and Torii, 2007). *SPCH* also has epistasis over *ERL1, ERL2,* and *TMM* during stomata development suggesting that *SPCH* acts downstream of these genes (MacAlister et al., 2007; Pillitteri and Torii, 2007). To further this hypothesis it has been shown that MPK3/6 can phosphorylate SPCH (Lampard et al., 2008))

The next transition in the stomatal development pathway, the cell fate transition from meristemoid to GMC, is regulated by the transcription factor MUTE. In *mute* no stomata are formed, instead meristemoids go through excessive amounts of asymmetrical divisions before arresting (Pillitteri et al., 2007). Overexpression of MUTE through the *CaMV 35S* promoter leads to almost all cells in the epidermis being converted into stomata (Pillitteri et al., 2008; Pillitteri et al., 2007). MUTE is transiently expressed in all organs that contain stomata and specifically is found in meristemoids, GMC and mature stomata (Pillitteri et al., 2008). In genetic crosses of *mute* with *tmm* and *er erl1 erl2* there appears to be a combination of phenotypes. In cotyledons both *tmm mute* and *er erl1 erl2 mute* plants have a very large increase of meristemoids but they do not differentiate into stomata indicating that *MUTE* acts downstream of the receptors (Pillitteri et al., 2008). However in stems *tmm* appears to have epistasis over *mute* indicating that TMM's promotion of stomata development in stems occurs without MUTE (Pillitteri et al., 2008).

The last step in the stomatal lineage, the symmetrical division of the GMC into two guard cells is controlled by the transcription factor FAMA. The *fama* mutation leads to excessive GC division that results in the production of long rows of GC-like cells, in essence GCs are prevented from differentiating and continue to divide forming rows of parallel cells (Ohashi-Ito and Bergmann, 2006). Overexpression of FAMA results in the epidermis being covered completely in kidney shaped cells similar in appearance to GCs (Ohashi-Ito and Bergmann, 2006). FAMA is expressed in GMCs and weakly expressed in GCs (Ohashi-Ito and Bergmann, 2006). Genetic interactions with *yda* and *fama*

revealed an additive phenotype with the formation of clustered rows of GC-like cells indicating that *FAMA* acts downstream of *YDA* (Ohashi-Ito and Bergmann, 2006).

Two paralogue transcription factors SCREAM/ICE1 and SCREAM2 are involved in the coordination and specificity of the chronological order of SPCH, MUTE and FAMA (Kanaoka et al., 2008). A constitutively active form of *SCRM (scrm-D)* has an epidermis made up completely of stomata. Double mutants with bHLH knockouts and *scrm-D* have interesting phenotypes as well. Thus, *mute scrm-D* have an epidermis made up of meristemoid like cells, indicating that all cells in a leaf entered the stomata development pathway but aborted differentiation during the meristemoid transition to GMC, the step that is under the control of *MUTE* (Kanaoka et al., 2008). This combination of phenotypes demonstrates that *scrm-D* is sufficient to enter the stomata development pathway but not sufficient to bypass the phenotype of *mute*.

The resulting phenotype of *fama scrm-D* has an epidermis consisting of large number of clustered rows of GC-like cells (Kanaoka et al., 2008). This result indicates that *SCRM* is able to start the stomatal development pathway without the presence of *MUTE* or *FAMA* and suggests that the function of SCRM depends on both.

In *spch scrm-D* the epidermis is void of stomata (Kanaoka et al., 2008). This epistasis of *spch* over *scrm-D* indicates that *SPCH* is required for entry to the stomata development pathway. Single mutant *scrm2* has no noticeable epidermal phenotype whereas the single mutant *scrm1* has only the occasional row of GC-like cells similar to *fama* which reveals redundancy of SCRM and SCRM2 and the fact that *SCRM* might

play a more significant role in regulation of GMC symmetric divisions (Kanaoka et al., 2008).

In the *scrm scrm2/+* line a phenotype similar to *mute* is observable with an epidermis consisting of aborted meristemoids which points to *SCRM2* being haploinsufficient to promote the conversion of the meristemoid into a GMC (Kanaoka et al., 2008).

Finally the double mutant *scrm scrm2* has a phenotype identical to *CA-YDA* and *spch* where the epidermis is completely empty of stomata lineage cells (Kanaoka et al., 2008) indicating that both *SCRM* and *SCRM2* are required for entry into the stomata development pathway. The similarities of phenotypes to the other bHLH transcription factors indicate potential interaction. Through yeast two hybrid and BiFC analysis it has been shown that SCRMand SCRM2 form heterodimers with SPCH, MUTE and FAMA, with preferential binding being shown towards SPCH (Kanaoka et al., 2008). Therefore all of the bHLH transcription factors are required to drive the stomatal development pathway from MMCs to meristemoids (SPCH), meristemoids to GMCs (MUTE), and GMCs to GCs (FAMA).

The other group of transcription factors currently known to affect the stomata lineage are the R2R3 MYB transcription factors, FLP and MYB88. These transcription factors are functionally redundant (Lai et al., 2005) and they act on the timing of the division of the GMC into two daughter GCs. The loss of function *MYB88* mutant displays no stomatal phenotype (Lai et al., 2005) and the *flp* phenotype consists of two

adjacent stomata with a small percentage of lone guard cells (Yang and Sack, 1995). In the double mutant *flp myb88* a phenotype similar to *fama* can be observed however the differentiation into GCs does take place to some degree (Lai et al., 2005). The similarity in phenotype could mean potential interaction with the bHLH transcription factors, however neither of the R2R3 MYB transcription factors have bHLH recognition sites nor has interaction between them been shown.

Conclusions

During early epidermis development (Fig 1.2), the ligand EPF2 binds to ER and TMM which initiates a MAPK signaling cascade by directly or indirectly activating YDA which inhibits the transcription factor SPCH and the formation of the meristemoid. Later EPF1 binds to ER and ERL1 which initiates the YDA MKK signaling cascade that potentially inhibits the transcription factor MUTE preventing the transition from meristemoid to GMC. TMM is required for EPF1 function but does not bind the ligand directly. STOMAGEN acts as an antagonist to the ERf receptors, inhibiting the signaling pathway. No known receptors have been found to inhibit FAMA and FLP and thus the phase transition from GMC to GCs may act in a time dependent fashion. Which receptors bind STOMAGEN is still in question and how the ERf interacts with TMM is still unknown. Nor has there been a connection made, either direct or indirect, between the ERf and YDA, leaving for a possibility of unknown intermediates between the two.

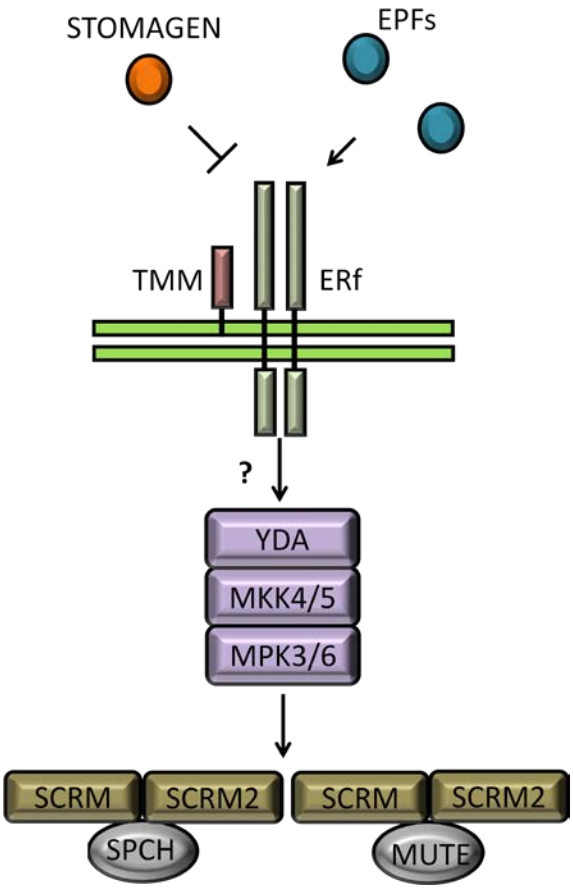

Figure 1.2 ERf signalling pathway

The STOMAGEN (antagonist) or EPFs (agonists) bind to the receptors TMM and ERfs. When activated by agonists, the ERf either directly or indirectly activates the YDA MAPK signaling cascade. The MAPK signaling cascade phosphorylates the transcription factor complexes of SCRM/SCRM2 SPCH and SCRM/SCRM2MUTE which inhibits stomata development.

GPI Anchors

In order to find new genes regulating stomata development an ethylmethylsulfate (EMS) induced mutant screen of *Arabidopsis thaliana* was performed. During the screen we isolated a mutant with stomata clusters. It was determined that the mutation occurred in the gene encoding the catalytic subunit of the Glycosylphosphatidylinositol **(**GPI) anchor transamidase complex.

GPI anchors are post translational modifications attached to proteins in the lumen of the endoplasmic reticulum. The core structure of GPI anchors consists of an ethanolamine phosphate (EtNP), three to four mannoses (man), a glucosamine (GlcN), a phosphatidylinositol (PI) and a lipid tail (Fig 1.3). The lipid tail of a GPI-anchor is inserted into the outer leaflet of the plasma membrane and is used to anchor the protein to the membrane. The biosynthesis of the GPI anchor is highly conserved among mammals, yeast, and plants and therefore it has been postulated that the function of the GPI anchors is also conserved (Seifert, 2011; Tiede et al., 1999). All GPI anchored proteins have two domains that are important for their localization, an N-terminus endoplasmic reticulum signal sequence and a C-terminus GPI anchor signal sequence. The biosynthesis of a GPI anchor is a multistep process that begins on the cytoplasmic side of the endoplasmic reticulum and ends in the luminal side where the GPI anchor is attached to a pro-protein. The completed GPI-anchored protein is then transferred to the Golgi apparatus for lipid remodeling before being sent to the plasma membrane.

Function of GPI anchors

GPI anchored proteins (GPI-APs) vary drastically in size and have been identified in all cell types and tissues (Nosjean et al., 1997). The function of GPI-APs also vary drastically, from enzymes that catalyze the removal of phosphate groups (Low, 1999), protective coats of *T. brucei* (Ferguson et al., 1999), and to orientation of cellulose microfibril (Roudier et al., 2005). Defects in the GPI anchor biosynthesis pathway are lethal, inferring that at least some GPI anchors are essential proteins for the viability of a cell and the organism (Gillmor et al., 2005; Leidich et al., 1994; Nozaki et al., 1999). GPI anchors allow proteins to be anchored to the plasma membrane, and phospholipases are able to cleave GPI anchors releasing the protein from the membrane. What the specific purpose of the GPI anchor is and why it is used instead of a simple transmembrane domain is still unknown.

There has been a lot of work done to try to identify the function of GPI anchors in mammals through analysis of the GPI-AP Thy-1. This research has shed some light onto how GPI anchors affect the structure and function of GPI-APs. Thy-1 is glycosylated and removal of the glycoslylation does not affect the ability of monoclonal antibody OX7 to recognize the protein. At the same time, the removal of Thy-1's GPI anchor with phosphotidylinositol specific phospholipase-C does dramatically reduce the binding of the OX7 antibody (Barboni et al., 1995). This experiment demonstrates that Thy-1's structure is more dramatically changed upon the removal of the GPI anchor in

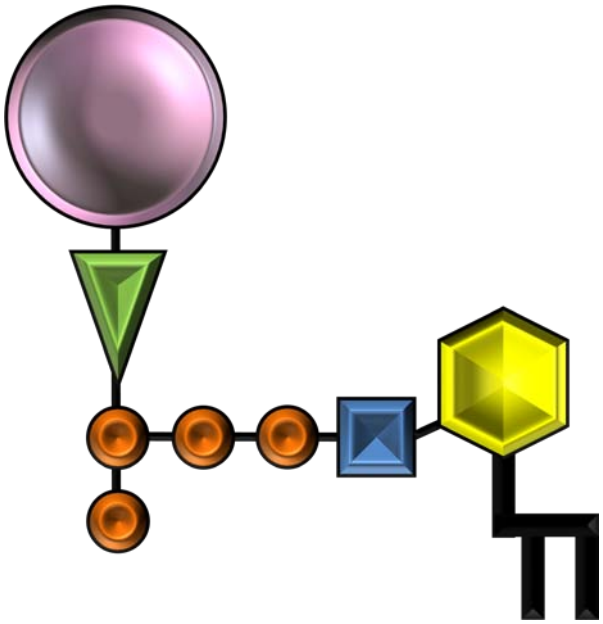

Figure 1.3 Core structure of a GPI anchor.

The core structure of a GPI consists of a phosphatidylinositol (yellow hexagon) attached to a glucosamine (blue square) followed by three to four mannoses (orange circles), and an ethanolamine phosphate (green triangle) linked to the third mannose. The C-terminal of the GPI anchored protein (pink circle) is attached to the ethanolamine phosphate and the lipid tail is attached to the phosphatidylinositol.

comparison to deglycosylation. This structural change is different enough that it prevents the binding of the monoclonal antibody OX7. To further test the ability of a GPI anchor to change the conformation of its attached protein circular dichroism was used on mouse and human Thy-1 after phospholipase-C and phospholipase-D treatments. After the removal of the GPI anchor, it was noted that there was no spectrum change in rat Thy-1 however there was a change in spectrum in human Thy-1 (Barboni et al., 1995). To see how big of a conformational change the loss of the GPI anchor causes monoclonal antibodies were raised against three different epitopes in Thy-1 and tested against soluble Thy-1. All three monoclonal antibodies were able to bind to native Thy-1 but were not able to bind to soluble Thy-1 (Kukulansky et al., 1999). These results indicate a major conformational change in Thy-1 after the release from the GPI anchor.

It is postulated that the GPI anchor is required for GPI-APs to associate with detergent resistant membranes referred to as "lipid rafts" (Jacobson et al., 2007; Schuck et al., 2004), although, the existence, size, and purpose of lipid rafts is still controversial (Tanner et al., 2011). Lipid rafts were first described as detergent resistant membranes that were able to withstand Triton-x 100 treatment at 4^{o}C. These membranes were determined to have a high content of sphingolipids, cholesterol, GPI-APs, and receptors. It has been proposed that the lipid domains of the GPI-anchored proteins allow for the close association towards lipid rafts, and GPI anchors are used to bring transmembrane receptors into lipid rafts. This phenomenon has been seen with Thy-1, where Thy-1 is required for the localization of Src family kinase (SFK) to lipid rafts (Rege et al., 2006).

At the same time, it was shown that the GPI anchor of Thy-1 was required for hep-1 induced SFK and FAK phosphorylation as a transmembrane version of Thy-1 prevented localization and phosphorylation of SFK and FAK (Rege et al., 2006). Whether the GPI anchor is mechanically involved in activating of kinases or if it is required just for the localization of proteins to lipid rafts is unknown.

GPI Anchor Biosynthesis

The biosynthesis of GPI anchors is a ten step process involving at least nineteen genes. The first step in the biosynthesis of a GPI anchor occurs on the cytoplasmic side of the endoplasmic reticulum and is responsible for the combination of UDP-GlcNAc with PI. The complex that catalyzes this reaction is composed of 6 different proteins in yeast and mammals (mammalian proteins shown in backets), Gpi3p (PIG-A), Gpi2p (PIG-C), Gpi15p (PIG-H), Gpi19p (PIG-P), Gpi1p (PIG-Q) and (DPM2) (Tiede et al., 1998; Watanabe et al., 2000; Yan et al., 2001). The newly formed GlcNAc-PI is then de-N-acylated by Gpi12p (PIG-L) (Watanabe and Kinoshita, 1999). An unknown flipase then transfers the de-N-acylated GlcNAc-PI to the luminal side of the endoplasmic reticulum. Inside the lumen, Gwt1p (PIG-W) acylates the inositol of the de-N-acylated GlcNaC-PI (Costello and Orlean, 1992; Urakaze et al., 1992).

The carbohydrate structure of the GPI anchor is composed of up to four mannoses derived from Dol-P-Man. Gpi14p and potentially Pbn1p (PIG-M and PIG-X) are responsible for the addition of the first mannose residue linked by an α1-4 bond to GlcN-

PI (Ashida et al., 2005; Davydenko et al., 2005). An EtNP side chain is then added to the first mannose residue by Mcd4p (PIG-N) (Gaynor et al., 1999; Hong et al., 1999). The second α1-6-linked mannose residue is added by Gpi18p (PIG-V) (Kang et al., 2005). The third α1-2-linked mannose residue is added by Gpi10p (PIG-B) (Sutterlin et al., 1998; Takahashi et al., 1996). An EtNP group is then added to the third mannose by Gpi13p and possibly Gpi11p (PIG-O and PIG-F) (Taron et al., 2000). The fourth α1-2-linked mannose residue is added by Smp3p (hSmp3/PIG-Z) to the third mannose (Grimme et al., 2001; Taron et al., 2004). The second mannose undergoes an EtNP addition by Gpi7p (hGpi7) and possibly Gpi11p (PIG-F) (Benachour et al., 1999; Shishioh et al., 2005; Taron et al., 2000). The completed GPI anchor is then ready for the next transamidation step.

GPI anchor Transamidation

Once the GPI anchor has been synthesized it is attached to the C-terminus of a pro-protein. The mature GPI-AP is sent to the Golgi apparatus and then to the plasma membrane. This process takes place on the luminal side of the endoplasmic reticulum and involves the GPI transamidase (GPI-T) complex consisting of three core subunits, Gpi8p (PIG-K), Gaa1p (GAA1), Gpi16p (PIG-T) and two loosely associated subunits, Gpi17p (PIG-S), and Gab1p (PIG-U) (Hong et al., 2003; Ohishi et al., 2001; Ohishi et al., 2000). The GPI-T is responsible for the cleavage of the pro-protein at a specific ω site

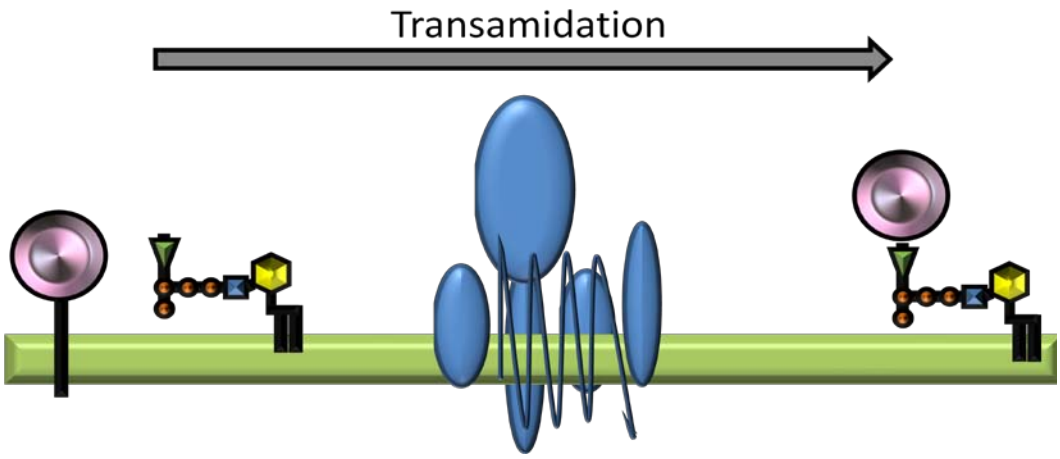

Figure 1.4 Attachment of GPI anchors

Inside the lumen of the endoplasmic reticulum, the pro-protein (pink circle) has a transmembrane domain (black rectangle). The pro-protein will bind to the GPI-T (blue components) and the GPI-T will cleave the transmembrane domain at the ω site. The GPI-T will then attach the GPI anchor to the protein creating the GPI anchored protein.

and the subsequent attachment of the GPI-anchor (Berger et al., 1988; Caras and Weddell, 1989; Chen et al., 2001) (Fig 1.4). Co-precipitation assays of the GPI-T complex show molecular weights larger than the combined sum of the subunits and could be postulated that there is at least two copies of each subunit in the complex (Ohishi et al., 2000). Gpi8p is the catalytic subunit of the GPI-T complex (Meyer et al., 2000). The other four subunits are also essential for the attachment of GPI anchors (Fraering et al., 2001; Hamburger et al., 1995; Hong et al., 2003; Ohishi et al., 2001). The loss of function of any of the subunits of the GPI-T is lethal (Benghezal et al., 1996; Ohishi et al., 2000).

Gpi8p

The catalytic subunit of the GPI-T complex is the 47 kDa protein Gpi8p. Gpi8p is predicted to have a single transmembrane domain with the majority of the protein localized to be inside the lumen of the endoplasmic reticulum. The sequence analysis of Gpi8p reveals homology to a novel family of cysteine proteases that are found in plants and invertebrates (Benghezal et al., 1996). Conditional knockdown mutants, in yeast, were able to grow normally at 25^{o}C but slower at 37^{o}C, while complete knockouts of Gpi8p were determined to be lethal through tetrad dissection (Benghezal et al., 1996). Human PIG-K is homologous to yeast Gpi8p and is able to rescue *gpi8-1 gpi7*, the conditional knockdown mutant (Benghezal et al., 1996). Analysis of point mutations has

determined that Gpi8p contains a histidine^{157}-cysteine^{199} catalytic dyad (Meyer et al., 2000; Ohishi et al., 2000). The mutation of other potential active sites in yGpi8p, Histidine 54 and Cysteine 85, led to partially functional mutants (Meyer et al., 2000). A low resolution structure of Gpi8p$^{24\text{-}337}$ has been resolved and the protein appears to fold in two domains, a large egg shaped domain that contains the catalytic machinery, and a small globular end. The two domains are linked by a long narrow stalk (Toh et al., 2011). One important finding of this structure was the discovery that cys85 (cys92 in PIG-K) is exposed to the solvent where it is able to form disulfide bonds with neighboring Gpi16p (Ohishi et al., 2003; Toh et al., 2011).

Closely associated with Gpi8p are Gpi16p and GAA1. Gpi16 has one predicted transmembrane domain and forms a direct disulfide bonds with Gpi8p (Ohishi et al., 2003). The function of Gpi16p could potentially be involved in the stabilization of Gpi8 as well as the addition of the GPI anchor to a GPI anchored protein (Fraering et al., 2001) (Ohishi et al., 2001). GAA1 associates with the catalytic subunit of the GPI-T. GAA1 does not show homology to any known proteins in the databases therefore it is difficult to hypothesize its specific function. Its luminal domain between the first and second transmembrane domain has been shown to be sufficient for interaction with the GPI-T complex (Ohishi et al., 2000) but yields a non-functional GPI-T (Vainauskas et al., 2002). The last two subunits, Gab1p and Gpi17p, have no known function and can bind together (Grimme et al., 2004). Gpi17p has been shown to have a strong interaction with the

GPI-T complex in humans (Ohishi et al., 2001) but is only weakly associated with the GPI-T complex in yeast (Zhu et al., 2005).

GPI anchor signal

The c-terminus of GPI-anchored proteins contains a GPI-anchor signal sequence that determines whether and where the GPI-T will cut the protein and attach the GPI anchor. The reaction takes place between residues that are referred to as the ω site and ω+1. This signal sequence is not conserved amongst species or even within a single species (Fankhauser and Maser, 2005). There are four conserved regions required for recognition of a GPI-AP by GPI-T (Fig 1.5). The first is a flexible stretch of polar amino acids from ω -11 to ω -1. The second is a short sequence of small residues at positions from ω -1 to ω +2 and including the ω site. In *H. sapiens* and *S. cerevisiae* typical ω amino acids are Gly, Ala, Ser, Asn, Asp, or Cys. The ω +1 position can be almost any amino acid. The ω +2 position is predominantly made up of Ala, Gly, or Ser (Eisenhaber et al., 1998; Eisenhaber et al., 2003a; Eisenhaber et al., 2004). The third region consists of a moderately polar spacer region from ω +3 to ω +8. The fourth region begins at ω +9 terminus of GPI-anchored proteins require a ΔG_{app} between -4 kcal mol^{-1} and 4 kcal mol^{-1} for the efficient cleavage and addition of a GPI anchor (Galian et al., 2012). This narrow range, between soluble and transmembrane proteins, could possibly mean that the pro-

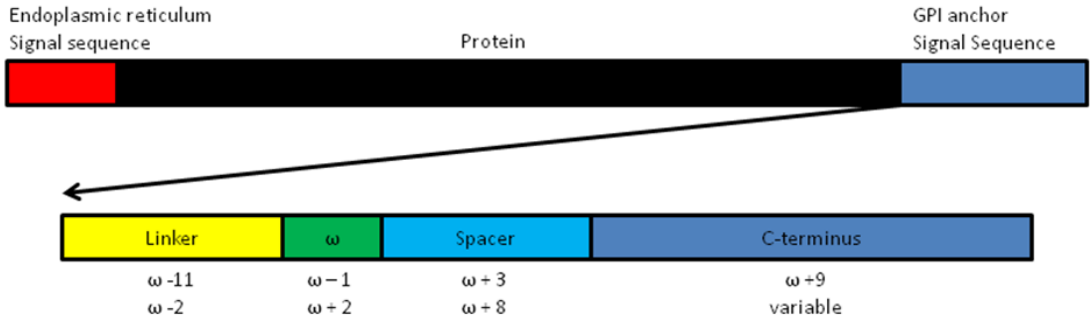

Figure 1.5 The GPI-anchor signal sequence

The GPI anchor signal sequence is found on the C-terminus of a GPI-AP. It consists of four domains: A linker domain (yellow), the ω domain (green), a spacer domain (light blue), and the C-terminus tail (dark blue).

protein can transition from a transmembrane form to a soluble form within the endoplasmic reticulum and that there is a certain degree of interdependence between the ω-site and the marginally hydrophobic C-terminus for recognition by the GPI-T (Galian et al., 2012).

GPI-anchor remodeling and transport to Golgi apparatus

After the attachment of the pro-protein to the GPI anchor by the GPI-T the GPI anchor undergoes a series of modifications and is processed through the Golgi before being sent to the plasma membrane. The mature GPI anchor of GPI-AP has at least four modifications. Mature GPI-anchors have an acyl-chain removed from the inositol in the endoplasmic reticulum by Bst1p in yeast and PGAP1 in mammals. The mature GPI-anchors contain a saturated fatty acid at the *sn*-2 position, for yeast the unsaturated fatty acid is removed and replaced by a C26:0 fatty acid (Fujita et al., 2006). Unlike yeast, the unsaturated fatty acid in mammals is removed and replaced with a C18:0 fatty acid (Maeda et al., 2007). In yeast, the diacylglycerol will sometimes be removed by Cwh43p and replaced by a ceramide, an occurrence that has not been reported in mammals (Umemura et al., 2007). The EtNP side chain on the second mannose is often missing in mature GPI-anchors. It's removal occurring in the endoplasmic reticulum of both yeast and mammals and may be a signal for the endoplasmic reticulum exit site recognition (Ferguson MAJ, 2008). Finally, β-GalNAc may be attached to the 4-position of the first mannose (Ferguson MAJ, 2008).

GPI-APs leave the endoplasmic reticulum through the endoplasmic reticulum exit sites (ERES). It has been hypothesized that correctly modified GPI-anchors act as endoplasmic reticulum exit signals (Doering and Schekman, 1996; Mayor and Riezman, 2004; McDowell et al., 1998)) as the inositol deacylation (Tanaka et al., 2004) and removal of the EtNP side chain from the second man (Fujita et al., 2009) are required for GPI-APs to enter the ERES in mammals. GPI-APs are loaded into coat protein complex II (COPII) vesicles through mediation by the p24 family of cargo proteins, type 1 transmembrane proteins that cycle between the endoplasmic reticulum and the Golgi (Fujita et al., 2011). The p24 protein family is responsible for connecting GPI-APs with SEC24C/D in mammals or Lst1p in yeast to allow for their export from the endoplasmic reticulum to the Golgi (Bonnon et al., 2010; Peng et al., 2000). Once in the Golgi, GPI-anchors undergo further lipid remodeling before being sent to the plasma membrane through clathrin-independent, dynamin-independent, Arf1 (mammals)/Cdc42 (yeast)-dependent pathways (Doherty and Lundmark, 2009; Howes et al., 2010).

GPI anchor biosynthesis genes in plants

Although the GPI-anchor biosynthesis pathway has been studied intensely in yeast and humans very little is known about the pathway in plants. In *Arabidopsis*, homologous genes exist for almost all the known components of GPI anchoring pathway

(Table 1.1) but currently the only genes that have been studied are *SETH1*, *SETH2*, and *PEANUT1*.

SETH1 encodes a putative phosphatidylinositol-glycan synthase subunit that has homology to Gpi2p, part of the complex involved in the first step of the GPI anchor biosynthesis pathway (Lalanne et al., 2004). *SETH2* encodes a putative GPI-GnT catalytic subunit homologous to Gpi3p. Analysis of *seth1* and *seth2* mutants revealed that these mutations are embryo lethal and a deficiency in GPI-anchor biosynthesis affects male gametophyte transmission (Lalanne et al., 2004). In *seth1* and *seth2* pollen grains develop normally but pollen tube germination and growth are drastically reduced in heterozygous tetrads (Lalanne et al., 2004). This means that GPI-APs play an important role during fertilization either for directional growth of pollen tubes or for female cue sensing.

PEANUT 1 (PNT1) encodes a putative mannosyltransferase with homology to the human PIG-M (Gillmor et al., 2005). As has been observed in *H. sapiens* and *S. cerevisiae* for other GPI anchor biosynthesis mutants, loss of function *pnt1* is embryo lethal. The mutation is recessive and segregates at less than 25% homozygous mutants upon selfing (Gillmor et al., 2005). The lower than expected segregation could be an indication of defects in fertilization of mutant gametes, results from *seth1 and seth2* hint at problems with pollen tube germination but embryo development cannot be dismissed off hand. The *pnt1* embryo undergoes delayed morphogenesis and abnormal cell divisions (Gillmor et al., 2005). Biochemical defects in *pnt1* show a lack of GPI-APs,

Table 1 Homology of proteins involved in the GPI anchor biosynthesis

All components of the GPI anchor biosynthesis pathway have homologues in *H. sapiens*, *S. cerevisiea*, and *A. thaliana*. Amino acid identity is shown for *A. thaliana*.

	H. sapiens	Identity	*S. cerevisiae*	Identity	*A. thaliana*
GlcNAc-PI synthesis	PIG-A	70%	Gpi3p	48%	SETH2
	PIG-C	33%	Gpi2p	21%	SETH1
	PIG-H	28%	Gpi15p	35%	At4G35530
	PIG-Pa	30%	GPI19p	27%	At2G39445
	PIG-Pb	33%	GPI19p	25%	At1G61280
	PIG-Q	37%	Gpi1p	25%	At3G57170
	PIG-Y	-	Eri 1p	-	nf
	DPM2	51%	nf	-	DPMS2
GlcNAc-PI De-N acytlation	PIG-La	34%	Gpi12p	33%	At2G27340
	PIG-Lb	34%	Gpi12p	33%	At3G58130
GPI flipping	?		?		?
Inositol acylation	PIG-W	29%	Gwt1p	36%	At4G17910
a1,4 Mannosyltransfer	PIG-M	41%	Gpi14p	39%	PNT1
	PIG-X	25%	Pbn1p?	44%	At5G46850
Etn-P transfer to Man-1	PIG-N	36%	Mcd4p	38%	At3G01380
a1,6 Mannosyltransfer	PIG-V	29%	Gpi18p	25%	At1G11880
a1,2 Mannosyltransfer	PIG-B	39%	Gpi10p	27%	At5G14850
Etn-P transfer to Man-3	PIG-O	38%	Gpi13p	35%	At5G17250
	PIG-F	41%	Gpi11p?	54%	At1G16040
a1,2 Mannosyltransfer	PIG-Z	25%	Smp3p	24%	At5G14850
Etn-P transfer to Man-2	hGpi7	37%	Gpi7p	35%	At2G22530
	PIG-F	41%	Gpi11p?	54%	At1G16040
GPI transamidase	PIG-K	54%	Gpi8p	60%	At1G08750
	GAA1	26%	Gaa1p	28%	At5G19130
	PIG-S	26%	Gpi17p	22%	At3G07180
	PIG-T	34%	Gpi16p	30%	At3G07140
	PIG-Ua	32%	Gab1p	28%	At1G63110
	PIG-Ub	30%	Gab1p	28%	At1G12730
Inositol deacylation	PGAP1	29%	Bst1p	30%	At3G27325

increased ectopic accumulation of xyloglucan, pectin and callose, and decreased cellulose. This information leads to the hypothesis that GAPs are required for the cell wall assembly (Gillmor et al., 2005). One further interesting discovery with *pnt1* was the mutant's ability to proliferate as callus (Gillmor et al., 2005). Since callus is undifferentiated growth, GAPs are required for coordinated differential growth within plants and could indicate they are needed for cell polarity.

Select GPI anchored proteins in plants

It has been computationally predicted that in *Arabidopsis thaliana* approximately 240 proteins are GPI-anchored (Borner et al., 2003; Borner et al., 2002; Eisenhaber et al., 2003b; Elortza et al., 2006). Of those proteins only 40 have been experimentally confirmed to have this modification. GPI-anchored proteins in *Arabidopsis* have a wide range of functions. The arabinogalactan family proteins (AGP) were some of the first GPI-APs to be experimentally confirmed to be GPI-anchored (Sherrier et al., 1999). Within the AGP family of there are also the Fasciclin-like AGPs (FLA), with *FLA4* regulating root growth under salt stress, and the Xylogen family (XYP), with *XYP1* and *XYP2* being involved in cell to cell communications during the development of the vasculature (Motose et al., 2004). *COBRA* (*COB*) encodes a GPI anchored protein that is involved in the polarization of cells during cellular expansion and is essential for cellulose deposition (Roudier et al., 2005). The *COBRA-LIKE* (*COBL*) genes make up a family of GPI anchored proteins that are involved in processes such as root tip growth

(Jones et al., 2006) and pollen tube growth (Lalanne et al., 2004; Li et al., 2013). *SKU5* is an abundant GPI-AP involved in root response to mechanical stimulation (Sedbrook et al., 2002)). *PMR6* encodes a GPI anchored protein involved in cell wall structure and powdery mildew susceptibility (Vogel et al., 2002).

Conclusions

The GPI anchor biosynthesis pathway has been well described in yeast and mammals, yet there are still many components with unknown functions. The purpose of the GPI anchor is poorly understood. There is evidence supporting a role in localization, conformation and potentially function of their associated GPI-APs.

In *A. thaliana* very little is known about GPI anchor biosynthesis and GPI-APs. The only three components of biosynthesis that have been described are embryo lethal which makes the comprehensive characterization of these mutants difficult. No components of the GPI-T complex have yet been discovered and characterized. Although there is homology to *H. sapiens* and *S. cerevisiae* it still is not certain if the GPI-T complex, in plants, functions in the same manner or not. It will be interesting to see what developmental processes require GPI-APs.

Chapter 2

Materials and Methods

Plant Materials and Growth Conditions

The *Arabidopsis* ecotype Columbia (Col) was used as the wild type. The mutant *atgpi8-1* was obtained from an EMS (ethyl methanesulfonic acid)-mutagenized (0.3% for 14h) screen in an *erl1-2 erl2-1* population (Shpak et al., 2004). Individual M2 seed lines were grown on modified Murashige and Skoog (MS) media plates supplemented with 1xGamborg B5 vitamins and 1% w/v sucrose and screened for stomata patterning defects in cotyledons. *Atgpi8-2* (CS853564) and *tmm-1* (CS6140) were obtained from the Arabidopsis Biological Resource Center (ABRC). The *erecta-105* mutant was described previously (Torii et al., 1996)). Plants were grown on a soil mixture of a 1:1 ratio of Promix PGX (Premier Horticulture Inc) and Vermiculite (Pametto Vermiculite Co) and where supplemented with Miracle-Gro (Scotts) and approximately 3.5mg/cm^3 of Osmocoat 15-9-12 (Scotts). All plants were grown at 20^{o}C under long-day conditions (18h light / 6h dark).

Map Based Cloning of atgpi8-1

A mapping population was created by crossing *atgpi8-1 erl1 erl2* to the Landsberg-*erecta* ecotype. A bulk segregant analysis (Lukowitz et al., 2000) using DNA

from 35 F2 *atgpi8-1*-like seedlings revealed linkage to the long arm of chromosome 1 between the SSLP markers NGA 280 and NGA 392. Fine mapping within this region using 961 F2 mutant plants localized the mutation between SSLP markers AW10 and AW18 in a segment of 172 kb which included two BACs (T27G7 and F22O13). Sequencing performed in this region identified a single G-A substitution at position 559bp from the ATG of the Atg108750 gene. The SSLP markers for map-based cloning were designed from the information provided by the Monsanto Arabidopsis Polymorphism and Ler Sequence Collection (http://www.Arabidopsis.org/Cereon/index.jsp) as well as the Arabidopsis Mapping Platform (http://amp.genomics.org.cn/). For primer sequences and amplified fragment sizes in both Col and Ler see Table 2.2.

Sequence alignment

Full length amino acid sequences of AtGPI8 homologs from *Saccharomyces cerevisiae* (GPI8; accession NP_010618) and *Homo sapiens* (PIG-K; accession CAI21820) were retrieved from NCBI database and aligned using ClustalW2 (http://www.ebi.ac.uk/Tools/msa/clustalw2/).

Table 2 SSLPs used to positionally clone *atgpi8-1*

Short sequence length polymorphisms (SSLP), Forward and reverse primers used to amplify SSLPs, expected size in Col and Ler (bp).

SSLPs	Forward primer	Reverse primer	Size of Col	Size of Ler
AW9	AAGAGCCTGTCACCAACTA	ATCGCAGATTACAAAACTAA	253	208
AW10	GGTAATCGCTAACTTTTTGT	GAATTTCAACCTGATGTTAT	198	178
AW13	GGTTAGGTTTTATTTCCAG	GTCATAGCCACAGTAGATG	203	169
AW17	TGTTTCACCAGCCTCCTCA	TTTGCTTTGTTCACCGACT	117	107
AW18	CAAGAAAGCAAGTCTTTTAT	AATGATCAGCGCCAAGCTAT	140	127

Crosses and Genotyping

To isolate *atgpi8-1*, M2 *atgpi8-1 erl1 erl2* was crossed to Col. The *atgpi8-1* plants were identified either by the short root phenotype of *atgpi8-1* or by genotyping. The primers AtGPI8 F1 (5`-GACTGGAGTTCCARCGTGG-3`) and AtGPI8 R1 (5'-GCAGAAGAACTCCAGAGTCACG-3`) were used to amplify a 1.5kb fragment of gDNA that contains a BsrFI restriction site in wt but was modified in *atgpi8-1*. Following restriction digestion and separation on a 1% agarose gel, wt has two 750bp bands and *atgpi8-1* has one 1.5kb band. The genotyping of *erl1* and *erl2* was performed as described by (Shpak et al., 2004).

For *atgpi8-1/atgpi8*-2 crosses, M3 *atgpi8-1* was crossed with *atgpi8-2/+*. The presence of *atgpi8*-1 was confirmed through genotyping. The presence of *atgpi8-2* was determined through PCR using the primer triplet AtGPI8 1780 (5`-GGTTGATACTTGCCAAGCTG-3`), AtGPI8 2171.rc (5` -GCTTCAGATTGGTGTATCTG-3'), and p745 (5`-AACGTCCGCAATGTGTTATTAAGTTGTC-3`) (Woody 2006). The wt allele results in one 400bp band and the *atgpi8-2* allele results in a 200bp band.

To generate *er atgpi8-1*, M3 *atgpi8-1* was crossed with *er-105*. The presence of *atgpi8-1* was confirmed through short roots and genotyping and the presence of *er-105* was determined by the phenotypes of short plant height, clustered inflorescence, and short blunt siliques.

To generate *tmm atgpi8-1*, M3 *atgpi8-1* was crossed to *tmm-1*. Short roots and genotyping, using the primers mentioned above, were used to identify *atgpi8-1* and stems lacking stomata were used to identify *tmm-1*.

Plants transformed with CA-YDA were selected through Basta spray (Finale, Bayer).

Reverse Transcription PCR

Total RNA was isolated from 12 day old Arabidopsis seedlings using Spectrum Plant Total RNA Kit (Sigma). First strand cDNA was synthesized from 785ng of RNA with ProtoScript M-MuLV Taq RT-PCR Kit (New England Biolabs) according to the manufacturer's instructions. PCR was performed with the first strand synthesized cDNA at 95^0C for 2mins, varying cycles of 95^0C for 30 seconds, 52^0C for 30 seconds and 72^0C for 30 seconds, followed by a final 72^0C for 5 minutes. The primers 5`-GGTTGATACTTGCCAAGCTG-3` and 5`-TCATCGTAGTAAAGATGATGAGACCATTAC-3` were used to amplify *ATGPI8* and the primers 5`-GCCATCCAAGCTGTTCTCTC-3` and 5`-GCTCGTAGTCAACAGCAACAA-3` were used to amplify *ACTIN* as a control. PCR products were separated on 1% agarose gel and visualized with ethidium bromide staining.

Analysis of plant development and growth

The stomatal index and stomata clustering were analyzed in cotyledons and leaves of 17 day old seedlings and stems and pedicels of mature plants using Differential Interference Contrast (DIC) microscopy. To analyze the effects of bikinin on stomata development seedlings were grown on MS plates supplemented with 30 µM bikinin (BK) for seven days. Plant tissues were fixed overnight in ethanol: acetic acid (9:1) and cleared in a chloral hydrate solution (chloral hydrate: water: glycerol 8:1:1) for approximately 24 hours. Structure of epidermis was observed using a Nikon Eclipse 80i microscope with DIC optics and pictures were obtained with a 12 megapixel cooled color DXM-1200c (Nikon) camera. Number of stomata were counted using NSI-Elements BR 2.30.

Morphometric data was collected at full maturity at 60 days for wild type and at 90 days for *atgpi8-1*. Plant height and distance between internodes were measured with a ruler. Length of pedicles was measured with digital calipers. C1 branching was determined by the number of cauline branches from the main stem. Seedlings were grown on vertical plates for root length measurements. To analyze callose accumulation seven day old seedlings were fixed overnight in a solution of ethanol: acetic acid (9:1), rinsed in 90% ethanol, incubated for 30 minutes in 0.09M sodium phosphate buffer (pH 9) and finally submerged for 1 hour in 0.01% aniline blue dissolved in the indicated buffer. A Nikon Eclipse 80i epifluorescence microscope with a 12 megapixel cooled

color camera and a UV-2A filter (Nikon) was used to observe the seedlings immediately after incubation.

Transient Transformation of Seedlings and Cell-to-Cell Mobility Assay

The transient transformation was performed with 1.1-μm tungsten M-17 microcarriers (Bio-Rad) fired at 400 psi using a PSD-1000/He particle bombardment system (Bio-Rad). The abaxial epidermis of seven day old Arabidopsis seedlings was transformed with the vectors pAVA 321 (CaMV 35S::mGFPS65T; (von Arnim et al., 1998)) and pAN456 (CaMV 35S::RFP with endoplasmic reticulum retention signal; (Nelson et al., 2007)). The fluorescence was observed 18 hours post-bombardment using a Zeiss Axio Observer.Z1 microscope and images were obtained with 1.3-megapixel cooled black and white ORCA-AG (Hamamatsu) camera. The presence of RFP designated transformed cells. Cell to cell mobility was established by analyzing GFP fluorescence.

Plasmid Construction

To create a construct with the yeast endoplasmic reticulum signal from yGpi8p joined to the rest of AtGPI8 PCR was performed on wt cDNA with primers GPI8 5' Bridge2 (5'- CAGGTGCAGATACGACTATCCACACAAAC-3') and GPI8 3' XhoI.rc (5'- TTCTCGAGTCATCGTAGTAAAGATGATGAGACC-3') to retrieve AtGPI8 cDNA minus the first 78bp. A linker region matching the last 6 base pairs of the 3' end

of the last 78bp of yeast GPI8 was added through the 5' primer and an XhoI restriction site was added by the 3' of primer. PCR was performed on yeast genomic DNA to retrieve the first 78bp (the ER signal sequence) of yeast GPI8 with primers yGPI8 5' XmaI (5'- CCCGGGATGCGTATAGCGATGCATCTGC-3') and yGPI8 3'bridge2.rc (5'- CTTACTACCCCTTTCAGGTGCAGATACGAC-3'). Primers added an XmaI site to the 5' end and a linker region matching the first 6 base pairs of the 5' end of the AtGPI8 fragment was added to the 3' end. Both fragments were combined through PCR, cut with XhoI and XmaI, and then ligated into p426 GPD (Mumberg et al., 1995) between bp 4340 and 4295. The sequence was confirmed through sequencing. There was a 1 base pair mutation T798→A798 but it does not cause a change in the amino acid sequence Thr → Thr.

Yeast transformation and tetrad dissection

A strain of BY4743 yeast with an insertion in GPI8/YDR331W (Thermo Scientific) was transformed with pMAB 202 through lithium acetate transformation (Becker). Transformants were selected on –URA plates and then transferred to sporulation liquid media (1% potassium acetate, 0.1% yeast extract, 0.05% dextrose) for 5 days at RT (Treco, 2008). 200ul of sporulated yeast were digested with zymolase (Bioworld), incubated at 30^{o}C for 10-15 minutes, diluted with 800µl of $_{dd}H_20$ and plated on thin 15% agar YPDA plates. Tetrads were examined and dissected using an Olympus BX41 microscope with a tetrad dissection micromanipulator attachment. The

heterozygous YDR331W strain was genotyped using primers: YGPI8-A (5`-ATAAATTAAACATGACCATAGCGGA-3`), YGPI8-B (5`-TAACAGCCTTATAAAGTTTTCCACG-3`) and YGPI8KanB (5`-CTGCAGCGAGGAGCCGTAAT-3`). PCR with primers YGPI8A and YGPI8B amplified a 679bp wt fragment and with primers YGPI8A and YGPI8KanB amplified a 597bp mutant fragment.

Arabidopsis Genome Initiative

Arabidopsis Genome Initiative numbers for the genes discussed here are as follows: *AtGPI8* (At1g08750), *ER* (At2g26330), *ERL1 (*At5g62230), *ERL2 (*At5g07180), *TMM (At1g80080*), and *YODA* (At1g63700).

Chapter 3

Results

Positional cloning of *atgpi8-1*

To advance our understanding of ERf/TMM signaling pathway, we searched for mutants containing stomata clusters in population of EMS mutagenized M2 *erl1 erl2* seedlings. That screen led to the identification of the 2094 mutant. Through map based cloning the location of the mutation was determined to be on the long arm of chromosome one between base pairs 2660266 and 2832207 (Fig. 3.1A). A sequence analysis of genes in this region uncovered a mutation in At1g08750 with a G to A substitution at base pair 559 which resulted in replacement of Arg_{42} to Gln_{42} (Fig. 3.1B). Homology analysis of At1g08750 revealed that the protein has a high amino acid sequence similarity to *S. cerevisiae* GPI8 (77%) and *H. sapiens* PIG-K (69%). *GPI8* and *PIG-K* encode the catalytic subunit of the glycosylphosphatidylinositol transamidase (GPI-T) that catalyzes the attachment of GPI-anchors to selected proteins in the endoplasmic reticulum. Analysis of available genome data suggests that the overall mechanism of GPI anchoring is conserved between plants, yeast and animals, as homologues for most essential genes are present (Eisenhaber et al. 2001 & 2003b). Since Arabidopsis contains only one gene with similarity to *GPI8/PIG-K*, At1g08750 is most certainly a catalytic subunit of plant GPI-T and thus we named the gene *AtGPI8* and the

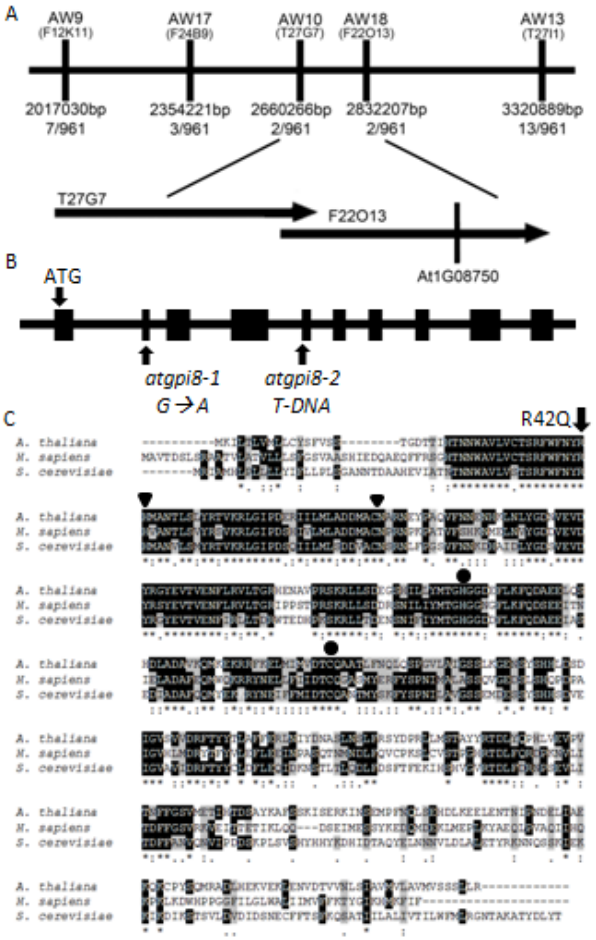

Figure 3.1 Positional cloning of *AtGPI8-1*

A. Fine mapping of *AtGPI8*. The *atgpi8-1* mutation was mapped to the upper arm of chromosome 1 between molecular markers AW9 and AW13. The number of recombinants obtained is indicated. Markers are positioned to scale. The corresponding BAC clones and the location of the *AtGPI8* locus (At1g08750) are indicated. B. The structure of *AtGPI8* gene and position of mutations. Boxes indicate exons and thick lines introns. G to A substitution in *atgpi8-1* results in Arg_{42}→Gln_{42}. Location of T-DNA insertion for *atgpi8-2* is shown. C. Alignment of Arabidopsis AtGPI8, *S. cerevisiae* GPI8 and *H. sapien* PIG-K predicted protein sequences. Identical residues are colored black, similar residues are colored gray. Residues labeled with an asterisk are conserved, while those labeled with a colon have conservation between groups of strongly similar properties. Residues labeled with a period have conservation between groups of weakly similar properties. Highly conserved residues examined by mutagenesis are marked by triangles. The conserved amino acids in predicted active sites are marked by circles. The position of the missense mutation in *atgpi8-1* is marked with an arrow.

mutation *atgpi8-1* (Fig. 3.1C). Although knockouts of GPI8 are lethal in *S. cerevisiae*, a mutation in a first conserved Histidine produces a partially functional GPI8 (Benghezal 1994)(Meyer et al., 2000)). The Arg_{42} to Gln_{42} mutation is one amino acid ahead of this residue. This mutation does not affect expression of the gene at the transcriptional level (Fig 3.2 G).

To confirm that the observed mutant phenotype is due to mutation in the *AtGPI8* gene, we performed allelic analysis using available T-DNA insertion line, CS853564 or *atgpi8-2*. The *atgpi8-2* mutant is distributed as a heterozygous line and it does not segregate out homozygous plants. Genotyping of 64 offspring of an *atgpi8-2+/-* plant identified 36% of *atgpi8-2+/-* and 66% of wt. For allelic analysis we crossed *atgpi8-1* with *atgpi8-2+/-* an*d* genotyped the F1 progeny. The identified *atgpi8-1/atgpi8-2* seedlings displayed a strong stomata clustering in cotyledons (Fig. 3.2A-D). In addition *atgpi8-1/atgpi8-2* plants were severely dwarfed, never flowered, and were unable to survive into maturity (Fig 3.2 E and F). This result confirmed that the positional cloning identified the mutation responsible for the phenotypes observed in *atgpi8-1*.

To investigate whether *AtGPI8* could rescue a yeast *gpi8* knockout mutant, we transformed a heterozygous GPI8 deficient yeast line (BY4743) with *AtGPI8* under the strong GPD promoter and with the yeast GPI8 endoplasmic reticulum signal sequence. Transformed and original BY4743 lines were sporulated and 60 tetrads were dissected

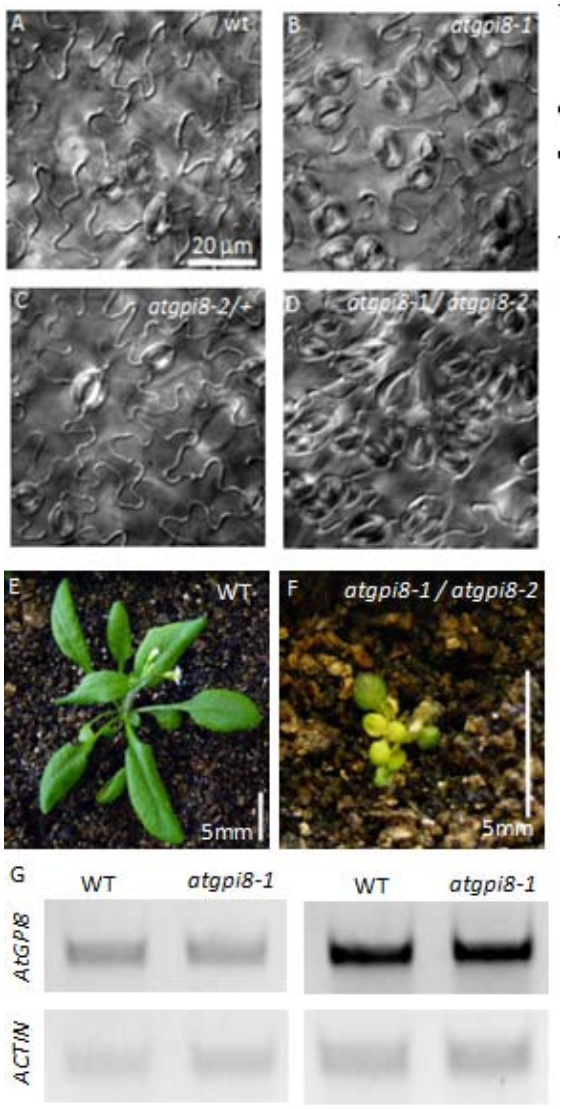

Figure 3.2 The *atgpi8-1* mutation leads to formation of stomata clusters and is allelic with *atgpi8-2*.

A-D. Cleared differential interference contrast images of abaxial epidermis of mature cotyledons of wt (A), *atgpi8-1* (B), *atgpi8-2*/+(C), and *atgpi8-1/atgpi8-2* (D). All images are under the same magnification. E and F. 30 day old plants of WT (E) and *atgpi8-1/atgpi8-2* (F). G. RT-PCR of *AtGPI8* at 31 (left panel) and 33 (right panel) cycles , and *ACTIN* control at 24 (left panel) and 25 cycles (right panel).

from each. For both lines no more than two of the four spores from a single tetrad were viable. We further genotyped ten spores from the transformed line and all confirmed to be wt. Thus, *AtGPI8* cannot rescue the yeast *gpi8* mutant which could be due to low level of ATGPI8 expression in yeast because of differences in codon usage or alternatively due to accumulated evolutionary differences in the structure and/or function of GPI8 in yeast and plants.

Atgpi8-1 mutations affect many developmental processes

The studies of mutations that disrupt the GPI anchoring process suggest that this protein modification is essential for early stages of organism development with mutants rarely surviving past embryogenesis (Gillmor et al., 2005; Lalanne et al., 2004; Leidich et al., 1994; Nozaki et al., 1999). The identification of the *atgpi8-1* mutation allowed us a unique opportunity to explore the importance of GPI anchoring during later stages of plant development. In *atgpi8*-1, the growth of above ground organs is very minimally affected early post germination with cotyledons and first rosette leaves being of similar size in the mutant and the wt (Fig 3.3 A-C). However, the root growth is significantly reduced in the mutant which is clearly obvious in 15 day old seedlings (Fig 3.3 A). Leaves formed later in development in *atgpi8-1,* are smaller, and at day 30 the wt and *atgpi8-1* plants noticeably differ in size (Fig 3.3 D and E). The *atgpi8-1* mutation also

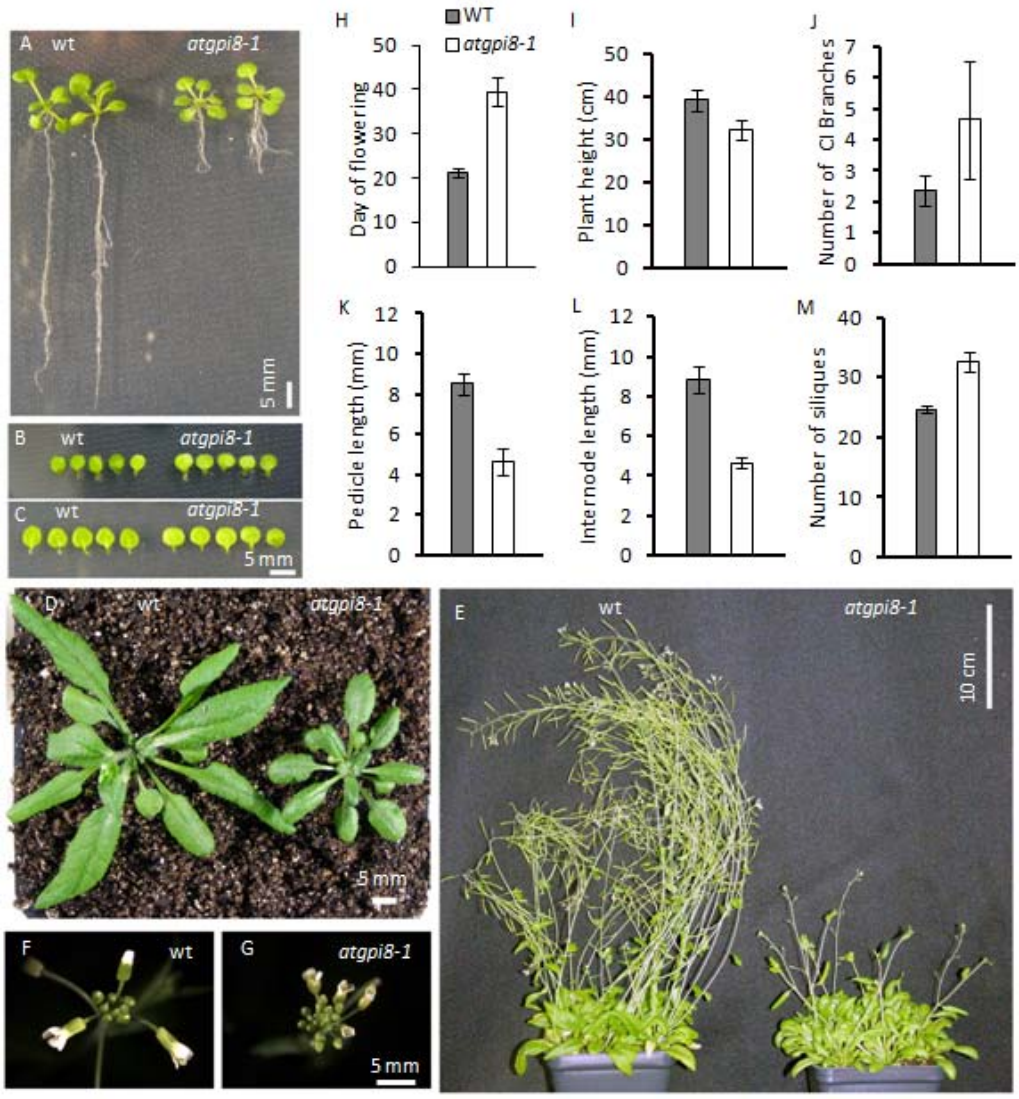

Figure 3.3 Growth phenotypes of *atgpi8-1* plants.

A-C. During seedling development the *atgpi8-1* mutation leads to reduced growth of roots and petioles (A) but not blades of cotyledons (B) or first two leaves (C). Images are of 15-days old seedlings. D and E. Size differences of 30 (D) and 60 (E) day old wt and *atgpi8-1* plants. F and G Inflorescences of wt and *atgpi8-1*. H-L. Morphometric analysis of wt (grey bars) and *atgpi8-1* (white bars) mature plants. H. Days until flowering (n = 20). I. Plant height (n=18). J. Number of RI branches (n=20) K. Length of pedicles (n = 40). L. Distance between pedicles (n = 40). M. Number of siliques on the main stem (n = 40). All values are mean ±SD.

leads to reduced internode and pedicel elongation which results in the formation of more compact inflorescence apices (Fig 3.3 F, G, K, L). At the same time the final height of *atgpi8-1* plants is only moderately reduced as number of internodes is increased (Fig 3.3 I, L). Increased number of C1 branching, the number of cauline branches on the main stem, in *atgpi8-1* suggest a decrease in the apical dominance (Fig 3.3 J). The transition to flowering in *atgpi8-1* is delayed with the mutant plants bolting at 39.5±3.3 days (±S.D here and below) versus at 21.1±1.1 days in wt (Fig 3.3 H).

In plants the GPI modification is essential for male fertility as evident from analysis of mutations in *PEANUT1*, *SETH1*, and *SETH2*, genes encoding GPI biosynthesis enzymes. The *seth1* and *seth2* mutants are male gamethophyte lethal and *peanut1* is seedling lethal with reduced pollen transmission (Gillmor et al., 2005; Lalanne et al., 2004). As the progeny of *atgpi8-2*+/- plants contained only 36% of heterozygotes and no homozygotes we investigated gametophyte viability using reciprocal crosses between wt and atgpi8-2+/-. The cross with *atgpi8-2* +/- as a male produced F1 progeny that was all wt (20 plants genotyped), suggesting that this mutation leads to male gametophyte lethality. The cross with *atgpi8-2* +/- as a female produced F1 that was 45% *atgpi8-2* +/- and 55% wt (20 plants genotyped), suggesting that atgpi8-2 mutation is not devastating for female gametophyte viability. At the same time, if the *atgpi8-2* mutation had an impact only on male gametophyte viability the *atgpi8-2*+/- plants should have segregated 50% heterozygotes instead of 36% (n=29). As we did not observe an increase in seed abortion in siliques of *atgpi8-2*+/- plants (average seed number per

silique were 35.8±3.8 for wt and 36.3±5.7 for *atgpi8-2*+/-; ±SD), and all seeds produced by atgpi8-2+/- plants germinated we speculate that the *atgpi8-2* mutation decreases viability of megaspore.

To evaluate gametophyte viability of *atgpi8-1* we examined the progeny of a heterozygous line distinguishing the mutants by their short root phenotype. As only 16.1% of *atgpi8-1*/+ progeny were mutants, which is significantly less than expected 25% (n=87; $p < 0.05$), we conclude that gametophyte viability is also reduced by the *atgpi8-1* mutation.

The analysis of *atgpi8* mutants implied that GPI anchored proteins play important roles in multiple developmental processes including lateral organ growth, apical dominance, and transition to flowering. In addition, GPI anchored proteins are not only essential for male gametophyte viability, but may also contribute to megaspore survival.

The *atgpi8-1* mutant has decreased plasmodesmata conductivity

The *atgpi8-1* was isolated as a mutant with substantial clustering of stomata (Fig 3.2 B). One of the potential causes of stomata cluster formation is an increase in plasmodesmata conductivity as in *chorus* and *kobito 1-3*, two mutants with stomata clustering and multiple other developmental defects (Guseman et al., 2010; Kong et al., 2012). Callose accumulation at the neck regions of plasmodesmata has a strong impact

on its conductivity with a decrease in callose deposition leading to plasmodesma opening (Guseman et al., 2010; Iglesias and Meins, 2000; Levy et al., 2007).

Aniline blue staining detected increased callose accumulation in *atgpi8-1*, which was particularly evident in vasculature and thick inner walls of guard cells (Fig 3.4 A and B). To examine whether the *atgpi8-1* mutation also has an impact on establishment of the proper size exclusion limit of plasmodesmata, we performed a cell to cell mobility assay. Two plasmids, one carrying a gene encoding GFP and the other a gene encoding endoplasmic reticulum localized RFP, both under control of 35S cauliflower mosaic virus (CaMV) promoter, were co-bombarded into the abaxial epidermis of seven day old seedlings. During bombardment, the particle gun always transforms an individual epidermal cell which can be confirmed by analysis of RFP expression as this protein cannot move to neighboring cells due to its endoplasmic reticulum retention. At the same time, if plasmodesmata are open the GFP can be detected in the surrounding cells due to its diffusion there through plasmodesmata. In wt seedlings we observed that in 85% of transformation events GFP was able to move to the neighboring cells, while GFP movement was not observed at all in *atgpi8-1* seedlings (Fig 3.4 C and D). The average cluster size of cells expressing GFP was 4.0±2.1 (±SD) for wt and 1.0±0 for *atgpi8-1*.

This data suggest that in *atgpi8-1* plasmodesmata conductivity is significantly decreased, thus the formation of stomata clusters cannot be caused by changes in the plasmodesmata structure. The decrease of plasmodesmata conductivity in *atgpi8-1* plants is not surprising as β-1,3- glucanases, enzymes degrading callose, are GPI anchored

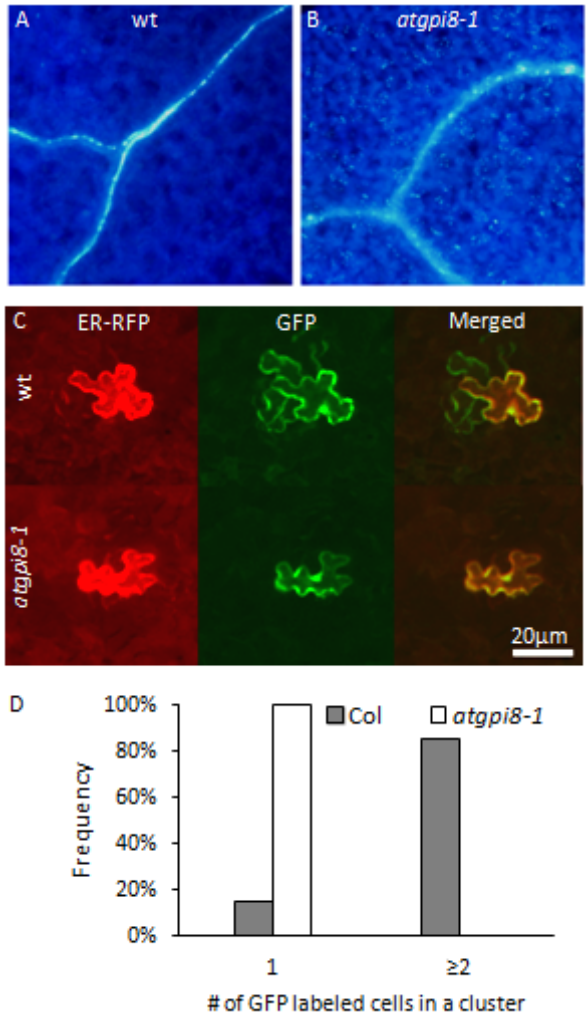

Figure 3.4 Increased callose accumulation and decreased plasmodesmata conductivity of *atgpi8-1*.

A and B, the accumulation of callose in seventeen day old cotyledons of *atgpi8-1* (B) is increased compared to wt (A) as determined by aniline blue staining. C and D, Analysis of GFP movement in the epidermis of seven day old seedlings suggests decreased plasmodesmata conductivity in *atgpi8-1*. C, representative images of the abaxial side of the epidermis expressing co-bombarded endoplasmic reticulum (ER) localized RFP (left), GFP (center) and both merged (right). D, distribution analysis of the number of cells in clusters expressing GFP from a single transformation event based on RFP expression; n = 40.

proteins (Elortza et al., 2006; Elortza et al., 2003) and mutation of AtBG_ppap, a plasmodesmata localized β-1,3-glucan synthase, increases callose accumulation and reduces plasmodesmata conductivity (Levy et al., 2007).

Synergistic interactions of *ERf*s and *ATGPI8* during stomata development

As GPI anchoring has not been linked with stomata development previously, we were especially interested in investigating the impact of the *atgpi8-1* mutation on epidermis differentiation. Analysis of epidermis in cotyledons, rosette leaves, stems, and pedicels demonstrated an increase in both the stomatal index (SI) and stomata clustering in *atgpi8-1* versus wt (Fig 3.5 A,B,C,G). The change in epidermis development is especially dramatic on the abaxial side of cotyledons and leaves with the SI being increased 2.5 times in *atgpi8-1* cotyledons and 2.3 times in *atgpi8-1* leaves. While less than 1% of stomata are in clusters in wt 72.2±6.3% and 33.9±8.9% of stomata are in clusters in abaxial epidermis of *atgpi8-1* cotyledons and rosette leaves, respectively. This data suggested the existence of a GPI anchored protein inhibiting stomata development. ERfs are plasma membrane localized receptors that are known to inhibit stomata development. To investigate whether a potential GPI anchored protein functions in ER signaling pathway we analyzed genetic interactions between mutants of *ERf* genes and *atgpi8-1*. In cotyledons and rosette leaves the stomata development was not changed by addition of *er* or *erl1 erl2* mutations to *atgpi8-1* possible because the stomatal phenotype of *atgpi8-1* was already very strong in those organs (Fig 3.5 A and B). Thus,

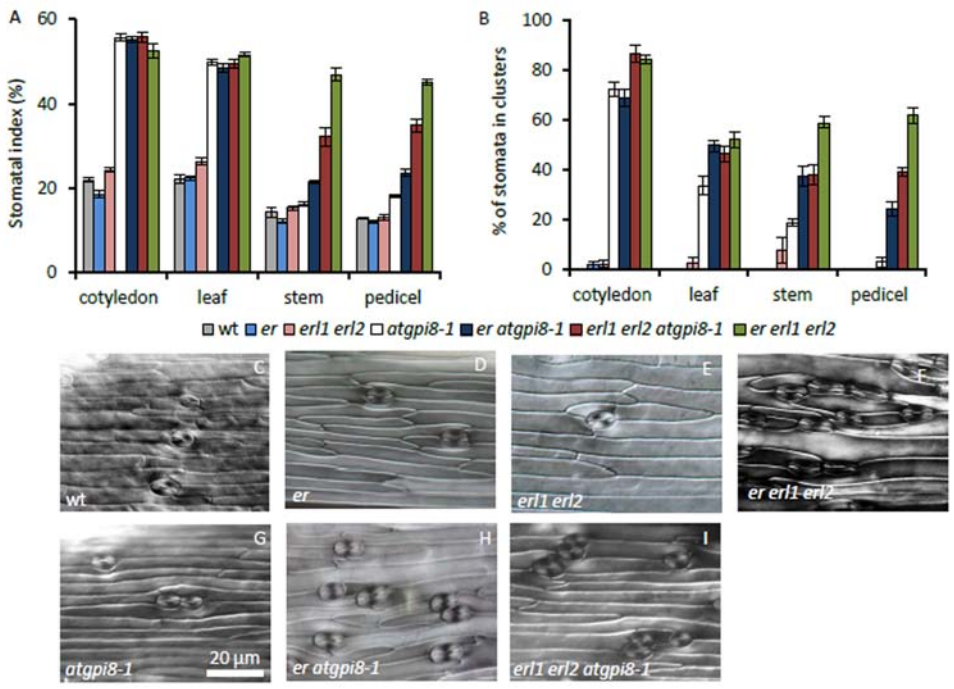

Figure 3.5 Genetic interactions of *ERECTA* family genes and *AtGPI8* during stomata development.

A and B, analysis of stomata formation in different organs of wt, *er*, *erl1 erl2*, *atgpi8-1*, *er atgpi8-1*, *erl1 erl2 atgpi8-1*, and *er erl1 erl2*. Stomatal index (A) and percent of stomata in clusters (B) were measured in the abaxial epidermis of mature cotyledons and first rosette leaf, as well as in the epidermis of stems and pedicels. Values are means ± SD; n=6. C-I, representative images of stem epidermis in wt, *er*, *erl1 erl2*, *er erl1 erl2*, *atgpi8-1*, *er atgpi8-1*, *and erl1 erl2 atgpi8-1*. All images are under the same magnification.

in cotyledons and rosette leaves the SI and the percent of stomata in clusters are identical in *atgpi8-1* and *er erl1* erl2 (Fig 3.5 A and B). However, in stems and pedicels where *atgpi8-1* phenotype was not so strong we observed synergistic interactions between *atgpi8-1* and *er* and between *atgpi8-1* and *erl1 erl2* (Fig 3.5 A-I). For example, in stems *atgpi8-1*, *er*, and *erl1 erl2* mutations do not increase SI on their own, but addition of *er* or *erl1 erl2* to *atgpi8-1* increases SI from 14.3±2.8% (±SD here and below) in the wt to 21.5±09% and 32.3±5.3%, respectively, (Fig 3.5 A-I). In pedicels of *atgpi8-1* only 3.2±4.9% of stomata are in clusters and no stomata clusters were detected in wt, *er*, or *erl1 erl2* pedicels. At the same time, pedicels of *atgpi8-1 er* and *atgp8-1 erl1 erl2* contained 24.3±7.1% and 39.4±9.2% of stomata in clusters, respectively. However, in stems and pedicels the synergistic interaction between *erl1 erl2* and *atgpi8-1* still does not increase the SI or the percent of stomata in clusters to the same level as in *er erl1 erl2* (Fig 3.5 A and B).

To further investigate the connection between GPI anchoring and ER signaling pathway, we analyzed genetic interactions of *ATGPI8* with *YODA (YDA)*, a MAPKK kinase functioning downstream of TMM and ERfs (Bergmann et al., 2004; Meng et al., 2012). The N terminus of YDA is a negative regulatory domain and its deletion produces a constitutively active YDA (CA-YDA) that inhibits stomata development and promotes stem and pedicel elongation when expressed in the wt (Bergmann et al., 2004). The CA-YDA construct was transformed into *atgpi8-1+/-* and then we analyzed stomata development in F2 progeny of a transgenic line selected based on observed changes in

plant morphology - increased length of pedicel and stem. The F2 progeny segregated CA-YDA in wt and *atgpi8-1/+* backgrounds as well as *CA-YDA atgpi8-1* plants. While in this particular line CA-YDA did not statistically significant change development of stomata on its own, it was able to rescue *atgpi8-1* plants decreasing both SI and stomata clustering in the mutant (Fig 3.6 A and B). Thus, the GPI anchored protein functioning in stomata development is upstream of YDA.

It has been previously reported that a GSK3 kinase regulates stomata development downstream of *TMM* and the *ERf* and upstream of *YDA* (Kim et al., 2012). To further validate the existence of a GPI anchored protein in the *ER* signaling pathway we examined whether bikinin, a GSK3 kinase inhibitor, could rescue the stomata phenotype of *atgpi8-1*. Similar to its effect on stomata development in *tmm* and *er erl1 erl2* bikinin decreased stomata index and stomata clustering in *atgpi8-1* seedlings (Fig 3.6 C-H). Growth in the presence of bikinin decreased stomatal index on the abaxial side of *atgpi8-1* cotyledons from 73±12% to 33±8% and stomata clustering from 70±14.8% to 16±12%. Thus, a GPI anchored protein is likely to function upstream of a GSK3 kinase.

Together all this data strongly suggests that a GPI-anchored protein regulating development of stomata functions in ERf signaling pathway upstream of MAP kinase cascade.

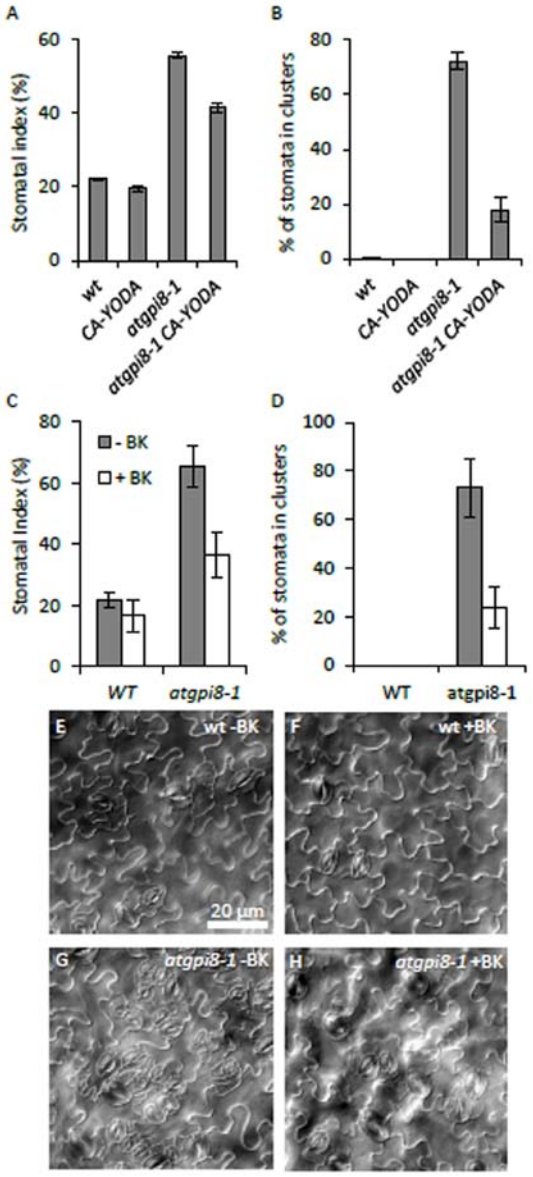

Figure 3.6 CA-YDA and bikinin partially rescue epidermal phenotype of *atgpi8-1*.

A and B. Expression of constitutively active YDA (CA-YDA) decreases stomatal index (A) and reduces percent of stomata in clusters (B) in abaxial epidermis of *atgpi8-1* mature cotyledons. Values are mean ± SD; n=8. C-D. The effect of 30 mM bikinin on stomatal index (C) and the percent of stomata in clusters (D) in abaxial epidermis of wt and *atgpi8-1* cotyledons. Values are mean ± SD; n=8. E-H. Representative images of abaxial epidermis of wt and *atgpi8-1* cotyledons grown on the control media (-BK) and media supplemented with bikinin (+BK).

The *tmm-1* mutation is epistatic to *atgpi8-1* mutation

A receptor like protein TMM forms heterodimers with ERfs (Lee et al., 2012). In contrast to ERfs which always inhibit stomata development TMM inhibits stomata development in cotyledons and leaves, but promotes it in stems and pedicels (Geisler et al., 1998). In order to understand the genetic interactions between TMM and the GPI-anchored protein involved in stomata development, we outcrossed *atgpi8-1* into the *tmm-1* mutant and analyzed SI and stomata clustering. In cotyledons and leaves *tmm-1* and *atgpi8-1* have very similar phenotypes: increased SI and massive stomata clustering, with only slightly weaker clustering of stomata in *atgpi8-1* (Fig 3.7 A and B). No additive effects of *the tmm-1* and *atgpi8-1* mutations were observed in leaves and cotyledons, and the phenotype of *atgpi8-1 tmm-1* was almost identical to phenotype of *tmm-1* (Fig 3.7 A-B). In stems and pedicels the phenotypes of *tmm-1* and *atgpi8-1* were quite different. There were no stomata formed in stems of *tmm-1* while in *atgpi8-1* stomata developed and they formed clusters (Fig 3.7 A-D). In the pedicels of *tmm-1,* a greatly reduced number of stomata were formed and no stomata clusters were observed (Fig 3.7 A and B). In contrast the pedicels of *atgpi8-1* had an increased SI and some stomata clustering (Fig 3.7 A and B). The phenotype of *atgpi8-1 tmm-1* epidermis in stems and pedicels was almost identical to *tmm-1* with almost complete stomata absence suggesting that *tmm-1* is epistatic to *atgpi8-1* (Fig 3.7).

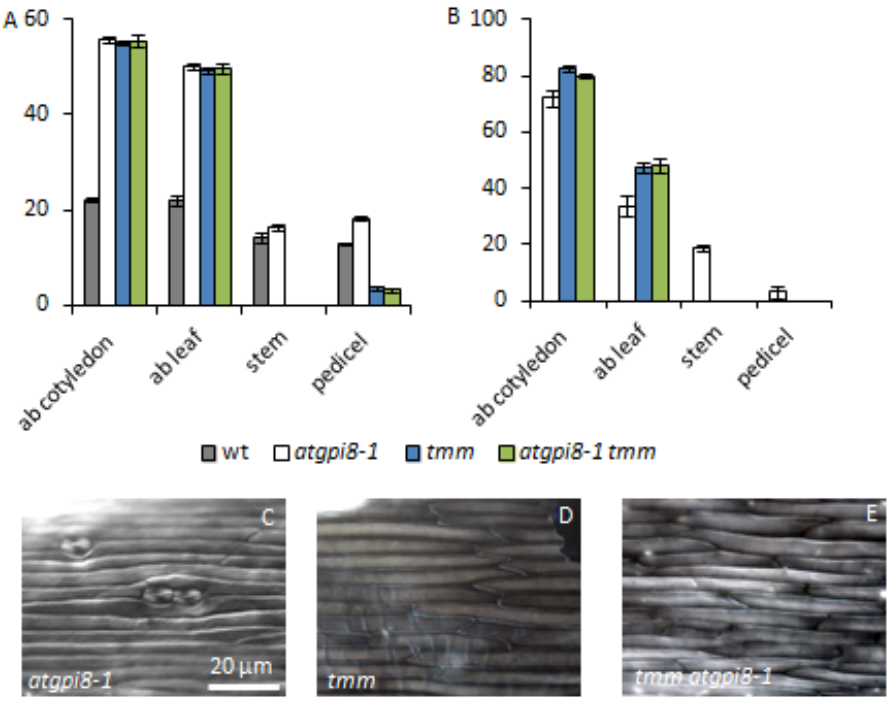

Figure 3.7 The *tmm-1* mutation is epistatic to the *atgpi8-1* mutation

A and B, analysis of stomata formation in different organs of wt, *atgpi8-1*, *tmm* and *atgpi8-1 tmm*. Stomatal index (A) and percent of stomata in clusters (B) were measured in the abaxial epidermis of mature cotyledons and first rosette leaf, as well as in the epidermis of stems and pedicels. Values are means ± SD; n=6. C-F Representative images of stem epidermis in *atgpi8-1*, *tmm*, *tmm atgpi8-1*. All images are under the same magnification.

Chapter 4

Discussion

In a genetic screen designed to discover new genes involved in the stomata development pathway we have found *atgpi8-1*, a mutation in the gene that encodes the catalytic subunit of the GPI-T complex with homology to Gpi8p in *S. cerevisae* and PIG-K in *H. sapiens*. The GPI-T complex is required for the removal of the C-terminus of GPI-APs and the attachment of the GPI anchor. As seen in *atgpi8-2*, a knockout of AtGPI8 is embryo lethal making experimentation difficult. The opportunity to analyze a partially functional mutation allows for observation of the many different processes GPI-APs are involved in, such as: fertility, root growth, delayed flowering, inflorescence architecture, apical dominance, plasmodesmata conductivity, and stomata development. There are currently confirmed GPI-APs that are known to affect fertility, root growth, and plasmodesmata conductivity. As well, *atgpi8-1* allows for a new system to study GPI anchoring mechanics in plants.

GPI-APs are involved in fertility

One of the issues that arise with *atgpi8-2*, and to a lesser extent with *atgpi8-1*, is the problem with fertility. Homozygous mutants of *atgpi8-2* are never formed, analyses of siliques show no aborted embryos, and *atgpi8-2* pollen is unable to fertilize wt plants. The pollen of *atgpi8-1* is also less efficient than wt as is seen in the progeny of *atgpi8-*

1+/- plants. This evidence suggests *atgpi8* mutant pollen is not viable. This is a strong indication that GPI-APs are required for male gamete formation and delivery to the ovule.

The first indication that GPI-APs were involved in fertility was with the discovery of the *seth1* and *seth2* mutants. These mutants demonstrated that a disrupted GPI anchor biosynthesis pathway prevents pollen tube germination. Further work has identified COBRA-LIKE 10 (COBL10) as a GPI-AP that plays a role in pollen tube germination and the pollen tube's ability to sense female gametophyte signaling cues (Li et al., 2013). Mutants of *cobl10* have reduced pollen tube growth and directional sensing is compromised. In wt, COBL10 is localized to the apical plasma membrane of pollen tubes and this localization was disrupted in *seth1-4* and *seth2* backgrounds. Therefore COBL10 and correctly functioning GPI anchors are required for proper pollen tube growth and female cue sensing.

Female embryo sacs, upon reception of pollen tubes, release cues to rupture the pollen tubes and allow the release of sperm. Once this has occurred the embryo sac no longer is able to attract further pollen tubes. This process involves the putative GPI-AP LORELEI. In *lorelei* mutants, pollen tubes do not rupture upon meeting the embryo sac and the arrival of the first pollen tube does not inhibit the attraction of more pollen tubes (Capron et al., 2008).

In regards to fertility, GPI-APs are not only involved in pollen tube growth but also in megaspore selection. Four megaspores are formed from a megaspore mother cell.

Of the four megaspores formed only one becomes a functional megaspore and the other three deteriorate without differentiating. AGP18 is a classical arabinogalactan protein that has been predicted to be GPI anchored (Demesa-Arevalo and Vielle-Calzada, 2013). It has been shown that AGP18 is required for the initiation of female gametogensis and for the selection of the functional megaspore (Demesa-Arevalo and Vielle-Calzada, 2013).

GPI-APs are involved in many different stages of fertilization. Pollen tube growth and germination was first shown to involve GPI-APs in the *seth1* and *seth2* mutants and further described in the *cobl10* mutant. The putative GPI-AP LORELEI is involved in the embryo sac recognition by pollen tubes. The megaspore selection is mediated by the GPI-AP AGP18. These results indicate the importance of GPI-APs during fertilization and how GPI anchoring is essential during reproduction.

GPI-APs are involved in root development

In *atgpi8-1* plants, the aerial organs are similar to wt. On the other hand, the roots of *atgpi8-1* are much shorter than wt. This observation suggests that the efficient GPI anchoring of proteins is required for root development.

The involvement of GPI-APs in root growth and development has been previously reported in *cobra* a mutant of the GPI-AP COBRA (COB) (Schindelman et al., 2001). COB is polarly localized and required for oriented cell expansion

(Schindelman et al., 2001). It has been shown that COB is expressed post-embryonically in the elongation zones of roots and hypocotyls but not in meristems (Roudier et al., 2005). COB is involved in cellulose microfibril deposition and is an important factor for cellulose synthesis (Roudier et al., 2005).

The GPI-AP SKU5 is structurally related to multiple-copper oxidases, although its function has not as of yet been elucidated, and is involved in root and hypocotyl mechanically stimulated growth. When grown vertically and rotated 30^{o} *sku5* roots begin to curl counterclockwise, even forming full loops. Hypocotyls grown in the dark also twisted more in a counter clockwise manner than wt. Furthermore, hypocotyls and roots in *sku5* are ten to fifteen percent shorter than wild type (Sedbrook et al., 2002).

In *cob* and *sku5* mutants, different degrees of decreased root growth are observed. This demonstrates the importance of multiple GPI-APs during development processes and even though the exact function of SKU5 is not yet known it could play a role in multiple functions.

GPI–APs are involved in regulation of plasmodesmata permeability

Reduced plasmodesmata conductivity in *atgpi8-1* could be caused by the inefficient GPI anchoring of at least two proteins: AtBG_ppap and PLASMODESMATA CALLOSE BINDING PROTEIN 1 (PDCB1).

Callose deposition and degradation acts as a gating mechanism to open and close plasmodesmata. The GPI-AP AtBG_ppap is the first β-1,3-glucanase enzyme observed to associate to plasmodesmata and to be involved in callose degradation. In T-DNA mutants of *AtBG_ppap* it has been shown that cell to cell movement of free GFP is reduced similar to that seen in *atgpi8-1*. The same mutants also demonstrate an increase in callose accumulation (Levy et al., 2007).

PDCB1 is a second GPI-AP (Elortza et al., 2003) localized to plasmodesmata (Simpson et al., 2009). PDCB1 contains an X8 domain that has callose binding activity. In hemizygous *35S::PDCB1* plants, cell to cell mobility of free GFP is reduced and callose accumulation is increased (Simpson et al., 2009). There has been no function prescribed to PDCB1 and exactly how it relates to the control of plasmodesmata is still unknown. It is interesting to find two proteins involved in the same process, with very similar phenotypes, and for both to be GPI anchored. This, combined with the analysis of *atgpi8-1*, indicates GPI-APs play an important role in callose mediated plasmodesmata gating.

GPI-APs are involved in stomata development

A prime candidate for the GPI-AP involved in stomata development is TMM. Originally TMM was predicted to contain a transmembrane domain (Nadeau and Sack, 2002a) however it has also been predicted to be GPI anchored (Borner et al., 2002)

Analysis of GFP localization in *TMM::GFP-TMM* and *TMM::TMM-GFP* plants also appears to indicate different localization with *GFP-TMM* in the plasma membrane and *TMM-GFP* difficult to determine precisely (Nadeau and Sack, 2002a). If TMM is GPI anchored then the C-terminus is cleaved and replaced by a GPI anchor. A GFP on the C-terminus therefore might be removed during this transamidation process. From the images available *TMM-GFP* does appear to be in the endoplasmic reticulum and the cytosol ((Nadeau and Sack, 2002a) and personal observation).

Two current GPI-AP prediction programs find a GPI anchor signal sequence at the C-terminus of TMM. BigPI predicts TMM to be GPI anchored with a p-value of 9.5e-05 with the ω site at S^{469} (Eisenhaber et al., 2003b). PredGPI predicts TMM to be GPI anchored with a specificity of 99.1% with the ω site at residue S^{467} (Pierleoni et al., 2008). The concurrence of both programs makes it highly probable that TMM is a GPI-AP.

TMM is a member of LRR-RLP family and has been shown to function with the ERf. The function of RLP in RLK signaling is still unknown and puzzling considering RLPs have no cytoplasmic domain (Jones and Jones, 1997). So far there have been 57 putative RLP genes identified (Wang et al., 2008) with only a handful having known function. Two of the LRR-RLPs with well studied functions are CLAVATA2 (Jeong et al., 1999) and TMM (Nadeau and Sack, 2002a). It has been proposed that RLPs required for development would have very close orthologoues in other plants. Nine

A. thaliana RLPs show a very high sequence similarity to RLPs from rice and could be developmental othologues (Fritz-Laylin et al., 2005).

Of the 57 putative LRR-RLPs, two have been predicted to be GPI-anchored: TMM and RLP29 (Borner et al., 2003; Borner et al., 2002). In the LysM-RLP family, two proteins, LYM1 and LYM2, have also been predicted to be GPI anchored. LYM1 and LYM2 are involved in plant defense and bind peptidoglucans, major components of bacterial cell walls (Willmann et al., 2011). It is still unknown if LYM1 and LYM2 have an interacting RLK partner.

The possibility of TMM being GPI anchored raises the question of how it interacts with the ERf receptors. There have been reports of mammalian c-Ret receptor kinase binding multiple GPI-APs. c-Ret receptor kinase interacts with at least four GPI-AP receptors: GFR α-1, GFR α-2, GFR α -3, and GFR α-4 (Trupp et al., 1998; Yang et al., 2007). The binding of the C-RET receptor to its GPI-AP partners is required for the binding of its ligand, glial cell line-derived neurotrophic factor (GDNF) (Trupp et al., 1998). Once the GFR family binds to c-Ret, they are able to correctly localize c-Ret to potential lipid rafts. This localization is essential for proper downstream signaling (Tansey et al., 2000).

The results from c-Ret receptor kinase demonstrates a precedence for GPI-APs that are able to bind to receptor kinases. This helps support the hypothesis that at least one GPI-AP is involved in the ERf signaling pathway. Microarray analysis of *scrm-D*

mute seedlings identified genes whose expression is deregulated when the epidermis of leaves consists only of meristemoids (*scrm-D mute*) (Pillitteri et al., 2011). Analysis of these genes reveals the highly expressed, predicted, GPI-APs: At1G80080 (*TMM)*, At2G25060, At2G28410, At2G34510, At3G07390, At4G31840, At5G40960, AT5G62210. However, none of the prospective mutants, besides *tmm*, that have been examined have shown a stomata phenotype (personal observations and correspondence).

If TMM is GPI anchored then why do we see different phenotypes in stems of *tmm* and *atgpi8-1*? This difference could be potentially explained a couple of different ways. The first possibility is TMM is a GPI-AP. In this scenario the different phenotype of *tmm* and *atgpi8-1* seen in stems can be explained by the availability of ligands. In leaves, the main ligands available to the ERf and TMM are EPF1, EPF2 and STOMAGEN. Stems, however, contain a large vascular structure in close proximity to the epidermis. This presents the possibility of CHALLAH escaping the vascular structure and leaking into the epidermis. In wt, CHALLAH is unable to bind to the ERf when TMM is present. Therefore, in *tmm* plants CHALLAH is able to leak to the epidermis, bind to the ERf, and inhibit stomata development. In *atgpi8-1* there are stomata in the stems because enough TMM is still being GPI anchored to prevent CHALLAH from inhibiting the ERf. The second possibility is TMM is available in two forms, a GPI anchored form and a transmembrane form, where the GPI anchored form of TMM inhibits stomata development and the transmembrane form promotes stomata development; with different expression levels of each form in leaves and stems. In *tmm*-

1 plants the lack of TMM in either form leads to clusters of stomata in leaves and a lack of stomata in stems, where in *atgpi8-1* the lack of a GPI anchored TMM leads to clusters of stomata in leaves and stems. The third possibility is TMM is not GPI anchored, instead the ERf and TMM interact with a currently unknown GPI-AP.

In order to elucidate if TMM is a GPI-AP there are two approaches currently underway. The first approach involves biochemical fractionation followed by treatment with phospholipase-C. Isolated crude membranes from *TMM::GFP-TMM* plants can be treated with phosphatidylinositol specific phospholipase-C. Phase separation, with Triton X114, can separate GPI-APs released from their anchors. Then a western blot with a GFP antibody can identify if TMM is GPI anchored. There are some potential problems with this biochemical approach: TMM is only expressed in developing meristemoids, GMC, and SLGCs (Nadeau and Sack, 2002a), and TMM may be a low abundance protein, similar to ERECTA (Shpak et al., 2003). Both of these issues could make the isolation and detection of TMM difficult.

The second approach is to replace TMM's predicted GPI anchor signal sequence with the known GPI anchor signal sequence from *COB* in one construct and with the transmembrane domain from ER in the other. This approach can provide evidence whether TMM can function with a GPI anchor or a transmembrane domain. The first approach can determine whether TMM is GPI anchored in vivo. The second approach will show whether TMM can function as a GPI-AP or with a transmembrane domain. It

can also confirm the hypothesis that TMM has different functions depending on how it is attached to the membrane.

A new model system for the study of GPI anchors

The possibilities proposed by analysis of *atgpi8-1*, in regards to GPI-APs, are exciting. This presents a new model system for the identification of GPI-APs, for the study of the GPI-T complex, and for the specificity of the ω site in *A. thaliana.*

As a new model system, *atgpi8-1* can be used to further proteomic studies in the identification of GPI-APs. The last proteomic studies done on GPI-APs in *A. thaliana* were performed over 10 years ago (Borner et al., 2003; Elortza et al., 2003) using phospholipase C and phospholipase D to cleave GPI-APs from their anchors. Using the same techniques, it is possible to perform similar experiments with WT to identify GPI-APs and then use *atgpi8-1* to confirm the results. The previous work also utilized callus tissue instead of seedlings. This could be problematic for the identification of GPI-APs in plants. GPI-APs are not required for growth as callus but are required for the growth of seedlings (Gillmor et al., 2005).

Differences in GPI anchor transamidation has already been noted between *A. thaliana* and other organisms, specifically in the GPI anchor signal sequence. Even within individual species there is no universal signal sequence. Work done with proteomic studies has helped identify differences in the signal sequence between *A. thaliana* and other species. The dominant residue for the GPI anchor signal sequence in

A. thaliana is proline (Eisenhaber et al., 2003b), the ω site is made of primarily of Serine with no GPI-APs being found to have a ω site consisting of Cysteine, and there is also a decreased amount of Leucine and increased amount of aromatic residues when compared to mammals (Eisenhaber et al., 2003b). There has also been a difference in lipid remodeling of GPI-APs reported in *A. thaliana* where it was observed that approximately 50% of AGPs have a β(1-4) galactose side chain at the 6-linked man of the core GPI anchor structure (Oxley and Bacic, 1999).

There are most likely further differences in the GPI anchor biosynthesis pathway, the GPI anchor signal sequence, and GPI anchor lipid remodeling that still have yet to be elucidated. Hopefully future endeavors to dissect these pathways will grant further insight on the effects of GPI anchored proteins in *A. thaliana.*

WORKS CITED

Abrash, E.B., and Bergmann, D.C. (2010). Regional specification of stomatal production by the putative ligand CHALLAH. Development *137*, 447-455.

Ashida, H., Hong, Y., Murakami, Y., Shishioh, N., Sugimoto, N., Kim, Y.U., Maeda, Y., and Kinoshita, T. (2005). Mammalian PIG-X and yeast Pbn1p are the essential components of glycosylphosphatidylinositol-mannosyltransferase I. Molecular biology of the cell *16*, 1439-1448.

Barboni, E., Rivero, B.P., George, A.J., Martin, S.R., Renoup, D.V., Hounsell, E.F., Barber, P.C., and Morris, R.J. (1995). The glycophosphatidylinositol anchor affects the conformation of Thy-1 protein. Journal of cell science *108 (Pt 2)*, 487-497.

Becker, D.M.a.L., V. Introduction of DNA into Yeast Cells. In Current Protocols in Molecular Biology.

Benachour, A., Sipos, G., Flury, I., Reggiori, F., Canivenc-Gansel, E., Vionnet, C., Conzelmann, A., and Benghezal, M. (1999). Deletion of GPI7, a yeast gene required for addition of a side chain to the glycosylphosphatidylinositol (GPI) core structure, affects GPI protein transport, remodeling, and cell wall integrity. The Journal of biological chemistry *274*, 15251-15261.

Benghezal, M., Benachour, A., Rusconi, S., Aebi, M., and Conzelmann, A. (1996). Yeast Gpi8p is essential for GPI anchor attachment onto proteins. The EMBO journal *15*, 6575-6583.

Berger, J., Howard, A.D., Brink, L., Gerber, L., Hauber, J., Cullen, B.R., and Udenfriend, S. (1988). COOH-terminal requirements for the correct processing of a phosphatidylinositol-glycan anchored membrane protein. The Journal of biological chemistry *263*, 10016-10021.

Bergmann, D.C. (2004). Integrating signals in stomatal development. Current opinion in plant biology *7*, 26-32.

Bergmann, D.C., Lukowitz, W., and Somerville, C.R. (2004). Stomatal development and pattern controlled by a MAPKK kinase. Science *304*, 1494-1497.

Bergmann, D.C., and Sack, F.D. (2007). Stomatal development. Annual review of plant biology *58*, 163-181.

Bonnon, C., Wendeler, M.W., Paccaud, J.P., and Hauri, H.P. (2010). Selective export of human GPI-anchored proteins from the endoplasmic reticulum. Journal of cell science *123*, 1705-1715.

Borner, G.H., Lilley, K.S., Stevens, T.J., and Dupree, P. (2003). Identification of glycosylphosphatidylinositol-anchored proteins in Arabidopsis. A proteomic and genomic analysis. Plant physiology *132*, 568-577.

Borner, G.H., Sherrier, D.J., Stevens, T.J., Arkin, I.T., and Dupree, P. (2002). Prediction of glycosylphosphatidylinositol-anchored proteins in Arabidopsis. A genomic analysis. Plant physiology *129*, 486-499.

Bowman, J.L. (1993). Arabidopsis: An Atlas of Morphology and Development ((New York: Springer-Verlag)).

Capron, A., Gourgues, M., Neiva, L.S., Faure, J.E., Berger, F., Pagnussat, G., Krishnan, A., Alvarez-Mejia, C., Vielle-Calzada, J.P., Lee, Y.R., *et al.* (2008). Maternal control of male-gamete delivery in Arabidopsis involves a putative GPI-anchored protein encoded by the LORELEI gene. The Plant cell *20*, 3038-3049.

Caras, I.W., and Weddell, G.N. (1989). Signal peptide for protein secretion directing glycophospholipid membrane anchor attachment. Science *243*, 1196-1198.

Chen, R., Knez, J.J., Merrick, W.C., and Medof, M.E. (2001). Comparative efficiencies of C-terminal signals of native glycophosphatidylinositol (GPI)-anchored proproteins in conferring GPI-anchoring. Journal of cellular biochemistry *84*, 68-83.

Costello, L.C., and Orlean, P. (1992). Inositol acylation of a potential glycosyl phosphoinositol anchor precursor from yeast requires acyl coenzyme A. The Journal of biological chemistry *267*, 8599-8603.

Davydenko, S.G., Feng, D., Jantti, J., and Keranen, S. (2005). Characterization of GPI14/YJR013w mutation that induces the cell wall integrity signalling pathway and results in increased protein production in Saccharomyces cerevisiae. Yeast *22*, 993-1009.

Demesa-Arevalo, E., and Vielle-Calzada, J.P. (2013). The Classical Arabinogalactan Protein AGP18 Mediates Megaspore Selection in Arabidopsis. The Plant cell *25*, 1274-1287.

Doering, T.L., and Schekman, R. (1996). GPI anchor attachment is required for Gas1p transport from the endoplasmic reticulum in COP II vesicles. The EMBO journal *15*, 182-191.

Doherty, G.J., and Lundmark, R. (2009). GRAF1-dependent endocytosis. Biochemical Society transactions *37*, 1061-1065.

Eisenhaber, B., Bork, P., and Eisenhaber, F. (1998). Sequence properties of GPI-anchored proteins near the omega-site: constraints for the polypeptide binding site of the putative transamidase. Protein engineering *11*, 1155-1161.

Eisenhaber, B., Maurer-Stroh, S., Novatchkova, M., Schneider, G., and Eisenhaber, F. (2003a). Enzymes and auxiliary factors for GPI lipid anchor biosynthesis and post-translational transfer to proteins. BioEssays : news and reviews in molecular, cellular and developmental biology *25*, 367-385.

Eisenhaber, B., Schneider, G., Wildpaner, M., and Eisenhaber, F. (2004). A sensitive predictor for potential GPI lipid modification sites in fungal protein sequences and its application to genome-wide studies for Aspergillus nidulans, Candida albicans, Neurospora crassa, Saccharomyces cerevisiae and Schizosaccharomyces pombe. Journal of molecular biology *337*, 243-253.

Eisenhaber, B., Wildpaner, M., Schultz, C.J., Borner, G.H., Dupree, P., and Eisenhaber, F. (2003b). Glycosylphosphatidylinositol lipid anchoring of plant proteins. Sensitive prediction from sequence- and genome-wide studies for Arabidopsis and rice. Plant physiology *133*, 1691-1701.

Elortza, F., Mohammed, S., Bunkenborg, J., Foster, L.J., Nuhse, T.S., Brodbeck, U., Peck, S.C., and Jensen, O.N. (2006). Modification-specific proteomics of plasma membrane proteins: identification and characterization of glycosylphosphatidylinositol-anchored proteins released upon phospholipase D treatment. Journal of proteome research *5*, 935-943.

Elortza, F., Nuhse, T.S., Foster, L.J., Stensballe, A., Peck, S.C., and Jensen, O.N. (2003). Proteomic analysis of glycosylphosphatidylinositol-anchored membrane proteins. Molecular & cellular proteomics : MCP *2*, 1261-1270.

Fankhauser, N., and Maser, P. (2005). Identification of GPI anchor attachment signals by a Kohonen self-organizing map. Bioinformatics *21*, 1846-1852.

Ferguson, M.A., Brimacombe, J.S., Brown, J.R., Crossman, A., Dix, A., Field, R.A., Guther, M.L., Milne, K.G., Sharma, D.K., and Smith, T.K. (1999). The GPI biosynthetic pathway as a therapeutic target for African sleeping sickness. Biochimica et biophysica acta *1455*, 327-340.

Ferguson MAJ, K.T., Hart GW (2008). Glycosylphosphatidylinositol membrane anchors (New York: Cold Spring Harbor Laboratory Press).

Fraering, P., Imhof, I., Meyer, U., Strub, J.M., van Dorsselaer, A., Vionnet, C., and Conzelmann, A. (2001). The GPI transamidase complex of Saccharomyces cerevisiae contains Gaa1p, Gpi8p, and Gpi16p. Molecular biology of the cell *12*, 3295-3306.

Fritz-Laylin, L.K., Krishnamurthy, N., Tor, M., Sjolander, K.V., and Jones, J.D. (2005). Phylogenomic analysis of the receptor-like proteins of rice and Arabidopsis. Plant physiology *138*, 611-623.

Fujita, M., Maeda, Y., Ra, M., Yamaguchi, Y., Taguchi, R., and Kinoshita, T. (2009). GPI glycan remodeling by PGAP5 regulates transport of GPI-anchored proteins from the ER to the Golgi. Cell *139*, 352-365.

Fujita, M., Umemura, M., Yoko-o, T., and Jigami, Y. (2006). PER1 is required for GPI-phospholipase A2 activity and involved in lipid remodeling of GPI-anchored proteins. Molecular biology of the cell *17*, 5253-5264.

Fujita, M., Watanabe, R., Jaensch, N., Romanova-Michaelides, M., Satoh, T., Kato, M., Riezman, H., Yamaguchi, Y., Maeda, Y., and Kinoshita, T. (2011). Sorting of GPI-anchored proteins into ER exit sites by p24 proteins is dependent on remodeled GPI. The Journal of cell biology *194*, 61-75.

Galian, C., Bjorkholm, P., Bulleid, N., and von Heijne, G. (2012). Efficient glycosylphosphatidylinositol (GPI) modification of membrane proteins requires a C-terminal anchoring signal of marginal hydrophobicity. The Journal of biological chemistry *287*, 16399-16409.

Gaynor, E.C., Mondesert, G., Grimme, S.J., Reed, S.I., Orlean, P., and Emr, S.D. (1999). MCD4 encodes a conserved endoplasmic reticulum membrane protein essential for glycosylphosphatidylinositol anchor synthesis in yeast. Molecular biology of the cell *10*, 627-648.

Geisler, M., Yang, M., and Sack, F.D. (1998). Divergent regulation of stomatal initiation and patterning in organ and suborgan regions of the Arabidopsis mutants too many mouths and four lips. Planta *205*, 522-530.

Gillmor, C.S., Lukowitz, W., Brininstool, G., Sedbrook, J.C., Hamann, T., Poindexter, P., and Somerville, C. (2005). Glycosylphosphatidylinositol-anchored proteins are required for cell wall synthesis and morphogenesis in Arabidopsis. The Plant cell *17*, 1128-1140.

Grimme, S.J., Colussi, P.A., Taron, C.H., and Orlean, P. (2004). Deficiencies in the essential Smp3 mannosyltransferase block glycosylphosphatidylinositol assembly and lead to defects in growth and cell wall biogenesis in Candida albicans. Microbiology *150*, 3115-3128.

Grimme, S.J., Westfall, B.A., Wiedman, J.M., Taron, C.H., and Orlean, P. (2001). The essential Smp3 protein is required for addition of the side-branching fourth mannose during assembly of yeast glycosylphosphatidylinositols. The Journal of biological chemistry *276*, 27731-27739.

Guseman, J.M., Lee, J.S., Bogenschutz, N.L., Peterson, K.M., Virata, R.E., Xie, B., Kanaoka, M.M., Hong, Z., and Torii, K.U. (2010). Dysregulation of cell-to-cell connectivity and stomatal patterning by loss-of-function mutation in Arabidopsis chorus (glucan synthase-like 8). Development *137*, 1731-1741.

Hamburger, D., Egerton, M., and Riezman, H. (1995). Yeast Gaa1p is required for attachment of a completed GPI anchor onto proteins. The Journal of cell biology *129*, 629-639.

Hara, K., Kajita, R., Torii, K.U., Bergmann, D.C., and Kakimoto, T. (2007). The secretory peptide gene EPF1 enforces the stomatal one-cell-spacing rule. Genes & development *21*, 1720-1725.

Hara, K., Yokoo, T., Kajita, R., Onishi, T., Yahata, S., Peterson, K.M., Torii, K.U., and Kakimoto, T. (2009). Epidermal cell density is autoregulated via a secretory peptide, EPIDERMAL PATTERNING FACTOR 2 in Arabidopsis leaves. Plant & cell physiology *50*, 1019-1031.

Hong, Y., Maeda, Y., Watanabe, R., Ohishi, K., Mishkind, M., Riezman, H., and Kinoshita, T. (1999). Pig-n, a mammalian homologue of yeast Mcd4p, is involved in transferring phosphoethanolamine to the first mannose of the glycosylphosphatidylinositol. The Journal of biological chemistry *274*, 35099-35106.

Hong, Y., Ohishi, K., Kang, J.Y., Tanaka, S., Inoue, N., Nishimura, J., Maeda, Y., and Kinoshita, T. (2003). Human PIG-U and yeast Cdc91p are the fifth subunit of GPI transamidase that attaches GPI-anchors to proteins. Molecular biology of the cell *14*, 1780-1789.

Howes, M.T., Mayor, S., and Parton, R.G. (2010). Molecules, mechanisms, and cellular roles of clathrin-independent endocytosis. Current opinion in cell biology *22*, 519-527.

Hunt, L., and Gray, J.E. (2009). The signaling peptide EPF2 controls asymmetric cell divisions during stomatal development. Current biology : CB *19*, 864-869.

Iglesias, V.A., and Meins, F., Jr. (2000). Movement of plant viruses is delayed in a beta-1,3-glucanase-deficient mutant showing a reduced plasmodesmatal size exclusion limit and enhanced callose deposition. The Plant journal : for cell and molecular biology *21*, 157-166.

Jacobson, K., Mouritsen, O.G., and Anderson, R.G. (2007). Lipid rafts: at a crossroad between cell biology and physics. Nature cell biology *9*, 7-14.

Jeong, S., Trotochaud, A.E., and Clark, S.E. (1999). The Arabidopsis CLAVATA2 gene encodes a receptor-like protein required for the stability of the CLAVATA1 receptor-like kinase. The Plant cell *11*, 1925-1934.

Jones, D., and Jones, J. (1997). The Role of Leucine-Rich Repeat Proteins in Plant Defences. In Advances in Botanical Research, pp. 89-167.

Jones, M.A., Raymond, M.J., and Smirnoff, N. (2006). Analysis of the root-hair morphogenesis transcriptome reveals the molecular identity of six genes with roles in root-hair development in Arabidopsis. The Plant journal : for cell and molecular biology *45*, 83-100.

Kagan, M.L., and Sachs, T. (1991). Development of immature stomata: evidence for epigenetic selection of a spacing pattern. Developmental biology *146*, 100-105.

Kanaoka, M.M., Pillitteri, L.J., Fujii, H., Yoshida, Y., Bogenschutz, N.L., Takabayashi, J., Zhu, J.K., and Torii, K.U. (2008). SCREAM/ICE1 and SCREAM2 specify three cell-state transitional steps leading to arabidopsis stomatal differentiation. The Plant cell *20*, 1775-1785.

Kang, J.Y., Hong, Y., Ashida, H., Shishioh, N., Murakami, Y., Morita, Y.S., Maeda, Y., and Kinoshita, T. (2005). PIG-V involved in transferring the second mannose in glycosylphosphatidylinositol. The Journal of biological chemistry *280*, 9489-9497.

Kim, T.W., Michniewicz, M., Bergmann, D.C., and Wang, Z.Y. (2012). Brassinosteroid regulates stomatal development by GSK3-mediated inhibition of a MAPK pathway. Nature *482*, 419-422.

Kondo, T., Kajita, R., Miyazaki, A., Hokoyama, M., Nakamura-Miura, T., Mizuno, S., Masuda, Y., Irie, K., Tanaka, Y., Takada, S., *et al.* (2010). Stomatal density is controlled by a mesophyll-derived signaling molecule. Plant & cell physiology *51*, 1-8.

Kong, D., Karve, R., Willet, A., Chen, M.K., Oden, J., and Shpak, E.D. (2012). Regulation of plasmodesmatal permeability and stomatal patterning by the glycosyltransferase-like protein KOBITO1. Plant physiology *159*, 156-168.

Kovtun, Y., Chiu, W.L., Tena, G., and Sheen, J. (2000). Functional analysis of oxidative stress-activated mitogen-activated protein kinase cascade in plants. Proceedings of the National Academy of Sciences of the United States of America *97*, 2940-2945.

Kukulansky, T., Abramovitch, S., and Hollander, N. (1999). Cleavage of the glycosylphosphatidylinositol anchor affects the reactivity of thy-1 with antibodies. Journal of immunology *162*, 5993-5997.

Lai, L.B., Nadeau, J.A., Lucas, J., Lee, E.K., Nakagawa, T., Zhao, L., Geisler, M., and Sack, F.D. (2005). The Arabidopsis R2R3 MYB proteins FOUR LIPS and MYB88 restrict divisions late in the stomatal cell lineage. The Plant cell *17*, 2754-2767.

Lalanne, E., Honys, D., Johnson, A., Borner, G.H., Lilley, K.S., Dupree, P., Grossniklaus, U., and Twell, D. (2004). SETH1 and SETH2, two components of the glycosylphosphatidylinositol anchor biosynthetic pathway, are required for pollen germination and tube growth in Arabidopsis. The Plant cell *16*, 229-240.

Lampard, G.R., Macalister, C.A., and Bergmann, D.C. (2008). Arabidopsis stomatal initiation is controlled by MAPK-mediated regulation of the bHLH SPEECHLESS. Science *322*, 1113-1116.

Lee, J.S., Kuroha, T., Hnilova, M., Khatayevich, D., Kanaoka, M.M., McAbee, J.M., Sarikaya, M., Tamerler, C., and Torii, K.U. (2012). Direct interaction of ligand-receptor pairs specifying stomatal patterning. Genes & development *26*, 126-136.

Leidich, S.D., Drapp, D.A., and Orlean, P. (1994). A conditionally lethal yeast mutant blocked at the first step in glycosyl phosphatidylinositol anchor synthesis. The Journal of biological chemistry *269*, 10193-10196.

Levy, A., Erlanger, M., Rosenthal, M., and Epel, B.L. (2007). A plasmodesmata-associated beta-1,3-glucanase in Arabidopsis. The Plant journal : for cell and molecular biology *49*, 669-682.

Li, S., Ge, F.R., Xu, M., Zhao, X.Y., Huang, G.Q., Zhou, L.Z., Wang, J.G., Kombrink, A., McCormick, S., Zhang, X.S., *et al.* (2013). Arabidopsis COBRA-LIKE 10, a GPI-anchored protein, mediates directional growth of pollen tubes. The Plant journal : for cell and molecular biology *74*, 486-497.

Low, M. (1999). GPI-anchored biomolecules—an overview. In GPI-anchored membrane proteins and carbohydrates a.I.S. Hoessli D. C., ed. (Austin, TX: Landes Company), pp. 1-14.

Lukowitz, W., Gillmor, C.S., and Scheible, W.R. (2000). Positional cloning in Arabidopsis. Why it feels good to have a genome initiative working for you. Plant physiology *123*, 795-805.

Lukowitz, W., Roeder, A., Parmenter, D., and Somerville, C. (2004). A MAPKK kinase gene regulates extra-embryonic cell fate in Arabidopsis. Cell *116*, 109-119.

MacAlister, C.A., Ohashi-Ito, K., and Bergmann, D.C. (2007). Transcription factor control of asymmetric cell divisions that establish the stomatal lineage. Nature *445*, 537-540.

Maeda, Y., Tashima, Y., Houjou, T., Fujita, M., Yoko-o, T., Jigami, Y., Taguchi, R., and Kinoshita, T. (2007). Fatty acid remodeling of GPI-anchored proteins is required for their raft association. Molecular biology of the cell *18*, 1497-1506.

Mayor, S., and Riezman, H. (2004). Sorting GPI-anchored proteins. Nature reviews Molecular cell biology *5*, 110-120.

McDowell, M.A., Ransom, D.M., and Bangs, J.D. (1998). Glycosylphosphatidylinositol-dependent secretory transport in Trypanosoma brucei. The Biochemical journal *335 (Pt 3)*, 681-689.

Meng, X., Wang, H., He, Y., Liu, Y., Walker, J.C., Torii, K.U., and Zhang, S. (2012). A MAPK Cascade Downstream of ERECTA Receptor-Like Protein Kinase Regulates Arabidopsis Inflorescence Architecture by Promoting Localized Cell Proliferation. The Plant cell.

Meyer, U., Benghezal, M., Imhof, I., and Conzelmann, A. (2000). Active site determination of Gpi8p, a caspase-related enzyme required for glycosylphosphatidylinositol anchor addition to proteins. Biochemistry *39*, 3461-3471.

Motose, H., Sugiyama, M., and Fukuda, H. (2004). A proteoglycan mediates inductive interaction during plant vascular development. Nature *429*, 873-878.

Mumberg, D., Muller, R., and Funk, M. (1995). Yeast vectors for the controlled expression of heterologous proteins in different genetic backgrounds. Gene *156*, 119-122.

Nadeau, J.A., and Sack, F.D. (2002a). Control of stomatal distribution on the Arabidopsis leaf surface. Science *296*, 1697-1700.

Nadeau, J.A., and Sack, F.D. (2002b). Stomatal development in Arabidopsis. The Arabidopsis book / American Society of Plant Biologists *1*, e0066.

Nelson, B.K., Cai, X., and Nebenfuhr, A. (2007). A multicolored set of in vivo organelle markers for co-localization studies in Arabidopsis and other plants. The Plant journal : for cell and molecular biology *51*, 1126-1136.

Nosjean, O., Briolay, A., and Roux, B. (1997). Mammalian GPI proteins: sorting, membrane residence and functions. Biochimica et biophysica acta *1331*, 153-186.

Nozaki, M., Ohishi, K., Yamada, N., Kinoshita, T., Nagy, A., and Takeda, J. (1999). Developmental abnormalities of glycosylphosphatidylinositol-anchor-deficient embryos revealed by Cre/loxP system. Laboratory investigation; a journal of technical methods and pathology *79*, 293-299.

Ohashi-Ito, K., and Bergmann, D.C. (2006). Arabidopsis FAMA controls the final proliferation/differentiation switch during stomatal development. The Plant cell *18*, 2493-2505.

Ohishi, K., Inoue, N., and Kinoshita, T. (2001). PIG-S and PIG-T, essential for GPI anchor attachment to proteins, form a complex with GAA1 and GPI8. The EMBO journal *20*, 4088-4098.

Ohishi, K., Inoue, N., Maeda, Y., Takeda, J., Riezman, H., and Kinoshita, T. (2000). Gaa1p and gpi8p are components of a glycosylphosphatidylinositol (GPI) transamidase that mediates attachment of GPI to proteins. Molecular biology of the cell *11*, 1523-1533.

Ohishi, K., Nagamune, K., Maeda, Y., and Kinoshita, T. (2003). Two subunits of glycosylphosphatidylinositol transamidase, GPI8 and PIG-T, form a functionally important intermolecular disulfide bridge. The Journal of biological chemistry *278*, 13959-13967.

Ohki, S., Takeuchi, M., and Mori, M. (2011). The NMR structure of stomagen reveals the basis of stomatal density regulation by plant peptide hormones. Nature communications *2*, 512.

Oxley, D., and Bacic, A. (1999). Structure of the glycosylphosphatidylinositol anchor of an arabinogalactan protein from Pyrus communis suspension-cultured cells. Proceedings of the National Academy of Sciences of the United States of America *96*, 14246-14251.

Peng, R., De Antoni, A., and Gallwitz, D. (2000). Evidence for overlapping and distinct functions in protein transport of coat protein Sec24p family members. The Journal of biological chemistry *275*, 11521-11528.

Pierleoni, A., Martelli, P.L., and Casadio, R. (2008). PredGPI: a GPI-anchor predictor. BMC bioinformatics *9*, 392.

Pillitteri, L.J., Bogenschutz, N.L., and Torii, K.U. (2008). The bHLH protein, MUTE, controls differentiation of stomata and the hydathode pore in Arabidopsis. Plant & cell physiology *49*, 934-943.

Pillitteri, L.J., Peterson, K.M., Horst, R.J., and Torii, K.U. (2011). Molecular profiling of stomatal meristemoids reveals new component of asymmetric cell division and commonalities among stem cell populations in Arabidopsis. The Plant cell *23*, 3260-3275.

Pillitteri, L.J., Sloan, D.B., Bogenschutz, N.L., and Torii, K.U. (2007). Termination of asymmetric cell division and differentiation of stomata. Nature *445*, 501-505.

Pillitteri, L.J., and Torii, K.U. (2007). Breaking the silence: three bHLH proteins direct cell-fate decisions during stomatal development. BioEssays : news and reviews in molecular, cellular and developmental biology *29*, 861-870.

Pillitteri, L.J., and Torii, K.U. (2012). Mechanisms of stomatal development. Annual review of plant biology *63*, 591-614.

Redei, G.P. (1962). Supervital Mutants of Arabidopsis. Genetics *47*, 443-460.

Rege, T.A., Pallero, M.A., Gomez, C., Grenett, H.E., Murphy-Ullrich, J.E., and Hagood, J.S. (2006). Thy-1, via its GPI anchor, modulates Src family kinase and focal adhesion kinase phosphorylation and subcellular localization, and fibroblast migration, in response to thrombospondin-1/hep I. Experimental cell research *312*, 3752-3767.

Roudier, F., Fernandez, A.G., Fujita, M., Himmelspach, R., Borner, G.H., Schindelman, G., Song, S., Baskin, T.I., Dupree, P., Wasteneys, G.O., *et al.* (2005). COBRA, an Arabidopsis extracellular glycosyl-phosphatidyl inositol-anchored protein, specifically controls highly anisotropic expansion through its involvement in cellulose microfibril orientation. The Plant cell *17*, 1749-1763.

Schindelman, G., Morikami, A., Jung, J., Baskin, T.I., Carpita, N.C., Derbyshire, P., McCann, M.C., and Benfey, P.N. (2001). COBRA encodes a putative GPI-anchored protein, which is polarly localized and necessary for oriented cell expansion in Arabidopsis. Genes & development *15*, 1115-1127.

Schuck, S., Manninen, A., Honsho, M., Fullekrug, J., and Simons, K. (2004). Generation of single and double knockdowns in polarized epithelial cells by retrovirus-mediated RNA interference. Proceedings of the National Academy of Sciences of the United States of America *101*, 4912-4917.

Sedbrook, J.C., Carroll, K.L., Hung, K.F., Masson, P.H., and Somerville, C.R. (2002). The Arabidopsis SKU5 gene encodes an extracellular glycosyl phosphatidylinositol-anchored glycoprotein involved in directional root growth. The Plant cell *14*, 1635-1648.

Seifert, C.L.a.G.J. (2011). Plant Plasma Membrane (Springer Berlin Heidelberg).

Sherrier, D.J., Prime, T.A., and Dupree, P. (1999). Glycosylphosphatidylinositol-anchored cell-surface proteins from Arabidopsis. Electrophoresis *20*, 2027-2035.

Shishioh, N., Hong, Y., Ohishi, K., Ashida, H., Maeda, Y., and Kinoshita, T. (2005). GPI7 is the second partner of PIG-F and involved in modification of glycosylphosphatidylinositol. The Journal of biological chemistry *280*, 9728-9734.

Shpak, E.D., Berthiaume, C.T., Hill, E.J., and Torii, K.U. (2004). Synergistic interaction of three ERECTA-family receptor-like kinases controls Arabidopsis organ growth and flower development by promoting cell proliferation. Development *131*, 1491-1501.

Shpak, E.D., Lakeman, M.B., and Torii, K.U. (2003). Dominant-negative receptor uncovers redundancy in the Arabidopsis ERECTA Leucine-rich repeat receptor-like kinase signaling pathway that regulates organ shape. The Plant cell *15*, 1095-1110.

Shpak, E.D., McAbee, J.M., Pillitteri, L.J., and Torii, K.U. (2005). Stomatal patterning and differentiation by synergistic interactions of receptor kinases. Science *309*, 290-293.

Simpson, C., Thomas, C., Findlay, K., Bayer, E., and Maule, A.J. (2009). An Arabidopsis GPI-anchor plasmodesmal neck protein with callose binding activity and potential to regulate cell-to-cell trafficking. The Plant cell *21*, 581-594.

Sugano, S.S., Shimada, T., Imai, Y., Okawa, K., Tamai, A., Mori, M., and Hara-Nishimura, I. (2010). Stomagen positively regulates stomatal density in Arabidopsis. Nature *463*, 241-244.

Sutterlin, C., Escribano, M.V., Gerold, P., Maeda, Y., Mazon, M.J., Kinoshita, T., Schwarz, R.T., and Riezman, H. (1998). Saccharomyces cerevisiae GPI10, the functional homologue of human PIG-B, is required for glycosylphosphatidylinositol-anchor synthesis. The Biochemical journal *332 (Pt 1)*, 153-159.

Takahashi, M., Inoue, N., Ohishi, K., Maeda, Y., Nakamura, N., Endo, Y., Fujita, T., Takeda, J., and Kinoshita, T. (1996). PIG-B, a membrane protein of the endoplasmic reticulum with a large lumenal domain, is involved in transferring the third mannose of the GPI anchor. The EMBO journal *15*, 4254-4261.

Tanaka, S., Maeda, Y., Tashima, Y., and Kinoshita, T. (2004). Inositol deacylation of glycosylphosphatidylinositol-anchored proteins is mediated by mammalian PGAP1 and yeast Bst1p. The Journal of biological chemistry *279*, 14256-14263.

Tanner, W., Malinsky, J., and Opekarova, M. (2011). In plant and animal cells, detergent-resistant membranes do not define functional membrane rafts. The Plant cell *23*, 1191-1193.

Tansey, M.G., Baloh, R.H., Milbrandt, J., and Johnson, E.M., Jr. (2000). GFRalpha-mediated localization of RET to lipid rafts is required for effective downstream signaling, differentiation, and neuronal survival. Neuron *25*, 611-623.

Taron, B.W., Colussi, P.A., Wiedman, J.M., Orlean, P., and Taron, C.H. (2004). Human Smp3p adds a fourth mannose to yeast and human glycosylphosphatidylinositol precursors in vivo. The Journal of biological chemistry *279*, 36083-36092.

Taron, C.H., Wiedman, J.M., Grimme, S.J., and Orlean, P. (2000). Glycosylphosphatidylinositol biosynthesis defects in Gpi11p- and Gpi13p-deficient yeast suggest a branched pathway and implicate gpi13p in phosphoethanolamine transfer to the third mannose. Molecular biology of the cell *11*, 1611-1630.

Tiede, A., Bastisch, I., Schubert, J., Orlean, P., and Schmidt, R.E. (1999). Biosynthesis of glycosylphosphatidylinositols in mammals and unicellular microbes. Biological chemistry *380*, 503-523.

Tiede, A., Schubert, J., Nischan, C., Jensen, I., Westfall, B., Taron, C.H., Orlean, P., and Schmidt, R.E. (1998). Human and mouse Gpi1p homologues restore glycosylphosphatidylinositol membrane anchor biosynthesis in yeast mutants. The Biochemical journal *334 (Pt 3)*, 609-616.

Toh, Y.K., Kamariah, N., Maurer-Stroh, S., Roessle, M., Eisenhaber, F., Adhikari, S., Eisenhaber, B., and Gruber, G. (2011). Structural insight into the glycosylphosphatidylinositol transamidase subunits PIG-K and PIG-S from yeast. Journal of structural biology *173*, 271-281.

Torii, K.U. (2012). Mix-and-match: ligand-receptor pairs in stomatal development and beyond. Trends in plant science *17*, 711-719.

Torii, K.U., Mitsukawa, N., Oosumi, T., Matsuura, Y., Yokoyama, R., Whittier, R.F., and Komeda, Y. (1996). The Arabidopsis ERECTA gene encodes a putative receptor protein kinase with extracellular leucine-rich repeats. The Plant cell *8*, 735-746.

Treco, D.A.a.W., F. (2008). Growth and Manipulation of Yeast. In Current Protocols in Molecular Biology.

Trupp, M., Raynoschek, C., Belluardo, N., and Ibanez, C.F. (1998). Multiple GPI-anchored receptors control GDNF-dependent and independent activation of the c-Ret receptor tyrosine kinase. Molecular and cellular neurosciences *11*, 47-63.

Umemura, M., Fujita, M., Yoko, O.T., Fukamizu, A., and Jigami, Y. (2007). Saccharomyces cerevisiae CWH43 is involved in the remodeling of the lipid moiety of GPI anchors to ceramides. Molecular biology of the cell *18*, 4304-4316.

Urakaze, M., Kamitani, T., DeGasperi, R., Sugiyama, E., Chang, H.M., Warren, C.D., and Yeh, E.T. (1992). Identification of a missing link in glycosylphosphatidylinositol anchor biosynthesis in mammalian cells. The Journal of biological chemistry *267*, 6459-6462.

Vainauskas, S., Maeda, Y., Kurniawan, H., Kinoshita, T., and Menon, A.K. (2002). Structural requirements for the recruitment of Gaa1 into a functional

glycosylphosphatidylinositol transamidase complex. The Journal of biological chemistry *277*, 30535-30542.

Vogel, J.P., Raab, T.K., Schiff, C., and Somerville, S.C. (2002). PMR6, a pectate lyase-like gene required for powdery mildew susceptibility in Arabidopsis. The Plant cell *14*, 2095-2106.

von Arnim, A.G., Deng, X.W., and Stacey, M.G. (1998). Cloning vectors for the expression of green fluorescent protein fusion proteins in transgenic plants. Gene *221*, 35-43.

Wang, G., Ellendorff, U., Kemp, B., Mansfield, J.W., Forsyth, A., Mitchell, K., Bastas, K., Liu, C.M., Woods-Tor, A., Zipfel, C., *et al.* (2008). A genome-wide functional investigation into the roles of receptor-like proteins in Arabidopsis. Plant physiology *147*, 503-517.

Wang, H., Ngwenyama, N., Liu, Y., Walker, J.C., and Zhang, S. (2007). Stomatal development and patterning are regulated by environmentally responsive mitogen-activated protein kinases in Arabidopsis. The Plant cell *19*, 63-73.

Watanabe, R., and Kinoshita, T. (1999). [Biosynthesis of GPI-anchored proteins and its deficiency]. Tanpakushitsu kakusan koso Protein, nucleic acid, enzyme *44*, 1329-1336.

Watanabe, R., Murakami, Y., Marmor, M.D., Inoue, N., Maeda, Y., Hino, J., Kangawa, K., Julius, M., and Kinoshita, T. (2000). Initial enzyme for glycosylphosphatidylinositol biosynthesis requires PIG-P and is regulated by DPM2. The EMBO journal *19*, 4402-4411.

Willmann, R., Lajunen, H.M., Erbs, G., Newman, M.A., Kolb, D., Tsuda, K., Katagiri, F., Fliegmann, J., Bono, J.J., Cullimore, J.V., *et al.* (2011). Arabidopsis lysin-motif proteins LYM1 LYM3 CERK1 mediate bacterial peptidoglycan sensing and immunity to bacterial infection. Proceedings of the National Academy of Sciences of the United States of America *108*, 19824-19829.

Yan, B.C., Westfall, B.A., and Orlean, P. (2001). Ynl038wp (Gpi15p) is the Saccharomyces cerevisiae homologue of human Pig-Hp and participates in the first step in glycosylphosphatidylinositol assembly. Yeast *18*, 1383-1389.

Yang, J., Runeberg-Roos, P., Leppanen, V.M., and Saarma, M. (2007). The mouse soluble GFRalpha4 receptor activates RET independently of its ligand persephin. Oncogene *26*, 3892-3898.

Yang, M., and Sack, F.D. (1995). The too many mouths and four lips mutations affect stomatal production in Arabidopsis. The Plant cell *7*, 2227-2239.

Zhu, Y., Fraering, P., Vionnet, C., and Conzelmann, A. (2005). Gpi17p does not stably interact with other subunits of glycosylphosphatidylinositol transamidase in Saccharomyces cerevisiae. Biochimica et biophysica acta *1735*, 79-88.

VITA

Mark Gerald Ronald Bundy was born on August 26th 1983 in Saskatoon, Saskatchewan, Canada to Kevin and Mary Bundy. After spending his first year in Saskatoon he then moved to Ottawa, Ontario. After completing High School at Bell High School he went to the University of Toronto for two years with a major in Celtic Archaeology. During this time he met a wonderful woman, Jessica, and moved to Tennessee to marry her. After completing the immigration process he attended the University of Tennessee in Knoxville where he completed his Bachelor's of Science in Biochemistry, Cellular, and Molecular Biology. In his senior year he began undergraduate research, in Dr. Elena Shpak's lab, studying stomata development. This experience prompted him to apply to the University of Tennessee's graduate school in order to continue this research. He is the father of two wonderful children, Morgan and Kieryn. In the little spare time that he does have he enjoys making medieval armor, sword fighting with his children, and day dreaming about sleep.